Developmental Biology 354 (2011) 87–101

Contents lists available at ScienceDirect

Developmental Biology

journal homepage: www.elsevier.com/developmentalbiology

EGFR signaling regulates cell proliferation, differentiation and morphogenesis during planarian regeneration and homeostasis

Susanna Fraguas, Sara Barberán, Francesc Cebrià *

Department of Genetics, Faculty of Biology, University of Barcelona and Institute of Biomedicine of the University of Barcelona (IBUB), Av. Diagonal 645, edifici annex planta 1, 08028 Barcelona, Catalunya, Spain

ARTICLE INFO

Article history:
Received for publication 13 December 2010
Revised 14 February 2011
Accepted 23 March 2011
Available online 31 March 2011

Keywords:
Planarian
Epidermal growth factor
Signaling pathway
Cell differentiation
Regeneration

ABSTRACT

Similarly to development, the process of regeneration requires that cells accurately sense and respond to their external environment. Thus, intrinsic cues must be integrated with signals from the surrounding environment to ensure appropriate temporal and spatial regulation of tissue regeneration. Identifying the signaling pathways that control these events will not only provide insights into a fascinating biological phenomenon but may also yield new molecular targets for use in regenerative medicine. Among classical models to study regeneration, freshwater planarians represent an attractive system in which to investigate the signals that regulate cell proliferation and differentiation, as well as the proper patterning of the structures being regenerated. Recent studies in planarians have begun to define the role of conserved signaling pathways during regeneration. Here, we extend these analyses to the epidermal growth factor (EGF) receptor pathway. We report the characterization of three epidermal growth factor (EGF) receptors in the planarian *Schmidtea mediterranea*. Silencing of these genes by RNA interference (RNAi) yielded multiple defects in intact and regenerating planarians. *Smed-egfr-1(RNAi)* resulted in decreased differentiation of eye pigment cells, abnormal pharynx regeneration and maintenance, and the development of dorsal outgrowths. In contrast, *Smed-egfr-3(RNAi)* animals produced smaller blastemas associated with abnormal differentiation of certain cell types. Our results suggest important roles for the EGFR signaling in controlling cell proliferation, differentiation and morphogenesis during planarian regeneration and homeostasis.

Introduction

The process of regeneration involves a complex interplay between cell proliferation, differentiation and patterning to ensure that correctly organized tissues are produced at the right time and in the right place. Since the signaling pathways that control these processes during normal development are well described, a key question is the extent to which the same pathways are involved in regeneration. Answering this question will not only provide insights into this fascinating biological phenomenon but also yield potential molecular targets for use in regenerative medicine.

Recent research has shown that pathways such as the transforming growth factor β (TGFβ)/bone morphogenetic protein (BMP), Notch, Wnt/β-catenin, Hedgehog, JAK/STAT, epidermal growth factor receptor (EGFR) and fibroblast growth factor receptor (FGFR) pathways are conserved in classical models of regeneration and may play critical roles in the regenerative process (Sánchez-Alvarado and Tsonis, 2006). One such model is the freshwater planarian, which has been the focus of increasing interest due to its remarkable regenerative capacity and a variety of characteristics that make it suitable for experimental manipulation (Agata et al., 2003; Newmark and Sánchez-Alvarado, 2002; Reddien and Sánchez-Alvarado, 2004; Saló, 2006). Planarian regeneration depends upon neoblasts, somatic pluripotent stem cells present in adult animals (Baguñà et al., 1989a; Newmark and Sánchez-Alvarado, 2000). Numerous studies have now begun to explore the role of the main signaling pathways during planarian regeneration. It has been shown, for instance, that the TGFβ/BMP pathway regulates dorsoventral polarity (Molina et al., 2007; Orii and Watanabe, 2007; Reddien et al., 2007), the Wnt/βcatenin and hedgehog pathways control anteroposterior polarity (Gurley et al., 2008; Iglesias et al., 2008; Petersen and Reddien, 2008; Rink et al., 2009; Yazawa et al., 2009) and the FGF receptor signaling pathway controls the spatial restriction of brain tissues in the head region (Cebrià et al., 2002a).

To gain further insights into the role of major signaling pathways in controlling planarian regeneration, we have begun to characterize the EGF receptor (EGFR) pathway. EGFRs are transmembrane receptors with tyrosine kinase activity that regulate multiple biological processes, including cell proliferation and differentiation. In mammals, the EGFR family comprises 4 receptors: EGFR, ErbB-2, ErbB-3 and ErbB-4. Through the binding of different ligands from the EGF family, this pathway plays an important role in the development of the CNS (Birchmeier, 2009; Wong and Guillaud, 2004; Xian and Zhou,

* Corresponding author. Fax: +34 934034420.
E-mail address: fcebrias@ub.edu (F. Cebrià).

0012-1606/$ – see front matter © 2011 Elsevier Inc. All rights reserved.
doi:10.1016/j.ydbio.2011.03.023

2004). In addition, overactivation of this pathway is common in many human cancers, which makes it an interesting therapeutic target (Burgess, 2008; Normanno et al., 2006). In *Caenorhabditis elegans*, *Drosophila melanogaster* and the platyhelminthes *Schistosoma mansoni* and *Echinococcus multilocularis* a unique homologue has been isolated (Aroian et al., 1990; Livneh et al., 1985; Shoemaker et al., 1992; Spiliotis et al., 2003). Previous studies have suggested that EGF could accelerate proliferation in planarians (Baguñà et al., 1989b). Here, we report the characterization of three EGFRs in the planarian *Schmidtea mediterranea*. Silencing of *Smed-egfr-1* results in decreased regeneration of eye pigment cells, abnormal pharynges and mouth openings, and development of non-lethal dorsal outgrowths. *Smed-egfr-3* silencing results in smaller blastemas and abnormal differentiation of the cephalic ganglia and certain cell types during regeneration. Taken together, our data show that the EGFR signaling pathway regulates multiple processes associated with cell differentiation and morphogenesis during planarian regeneration.

Material and methods

Animals and gene nomenclature

S. mediterranea from the clonal line BCN-10 were used for all experiments. Animals were maintained as described (Molina et al., 2007). Genes and RNAi experiments were named using the nomenclature proposed by Reddien et al. (2008).

Gene cloning and phylogenetic analysis

The amino acid sequences of EGFRs from vertebrates and invertebrates were used to carry out tblastn searches on the *S. mediterranea* genome assembly (v3.1, Washington University Sequencing Center, available at http://www.genome.wustl.edu). Several contigs corresponding to three different genes were isolated. Specific primers were used to amplify those sequences from cDNA. Subsequent 3′ and 5′ RACE yielded partial sequences for the three EGFR homologues, missing the 5′ ends. Similar searches and cloning strategies were used to clone *Smed-tph* (tryptophan hydroxylase), *Smed-th* (tyrosine hydroxylase) and *Smed-AGAT1* (Eisenhoffer et al., 2008). GenBank accession numbers for the genes reported here are: *Smed-th* HM777014, *Smed-tph* HM777015, *Smed-egfr-1* HM777018, *Smed-egfr-2* HM777017 and *Smed-egfr-3* HM777016.

For phylogenetic analyses, the tyrosine kinase domain from genes belonging to different families within this superfamily of receptors were obtained from pfam (Finn et al., 2010) and aligned with ClustalW2 (Larkin et al., 2007). A neighbor-joining tree was constructed using MEGA4 software (Tamura et al., 2007).

In situ hybridization

Whole-mount in situ hybridizations were performed as previously described (Molina et al., 2007; Umesono et al., 1997) using an Intavis InsituPro hybridization robot. For fluorescence in situ, samples were fixed and developed as previously described (Cebrià et al., 2007; Pearson et al., 2009) using Tyramide Signal Amplification (Perkin Elmer) according to the manufacturer's instructions. After in situ development, some animals were fixed in 4% PFA for 1 h at RT, blocked in 1% BSA in PBSTx (PBS containing 0.3% Triton X-100) and incubated with VC-1 antibody. All samples were observed through a Leica MZ16F stereomicroscope and images were captured with a ProgRes®C3 camera (Jenoptik). Confocal laser scanning microscopy was performed with a Leica SP2. After whole-mount in situ hybridization, some samples were embedded in a gelatin/albumin mixture and solidified with glutaraldehyde before preparing 30 μm transverse sections with a vibratome (Vibratome 1000 plus). A dose of 100 Gy was used in irradiation experiments, and animals were fixed and hybridized at the indicated time points.

RNAi

Double-stranded RNAs (dsRNA) for *Smed-egfr-1*, *Smed-egfr-2* and *Smed-egfr-3* were synthesized and delivered as described elsewhere (Sánchez-Alvarado and Newmark, 1999). Control animals were injected with water or dsRNA for GFP. In experiments involving more than one round of dsRNA injection and amputation, 3–4 days elapsed between each round of injection/amputation. For experiments in intact planarians, animals were injected for 3 consecutive days, cultured for 2 weeks and then re-injected on 3 more days. All animals were injected ventrally at different pre- and post-pharyngeal positions to rule out the possibility that the defects observed were related to the wounding produced by the injection. To avoid off-target effects of RNAi and confirm the specificity of the phenotypes observed, two different, non-overlapping regions of each *Smed-egfr-1* and *Smed-egfr-3* were used to synthesize dsRNA. For each gene, both dsRNA yielded the same phenotypes. The efficiency of RNAi silencing was checked by in situ hybridization (see Fig. S1). Combinatorial RNAi between the different planarian EGFRs did not generate synergistic or additional phenotypes to those observed after single RNAi. *Smed-egfr-2*(*RNAi*) did not yield any phenotype.

Immunostaining

Immunostainings were carried out as described elsewhere (Cebrià and Newmark, 2005). The following antibodies were used: VC-1, specific for planarian photosensitive cells (diluted 1/15,000, Sakai et al., 2000); anti-SYNORF1, specific for synapsin and used as a pan-neural marker (diluted 1/50, Developmental Studies Hybridoma Bank); anti-SMED-βCAT2, used to label the pharyngeal epithelial cells (diluted 1/1000, Chai et al., 2010); TMUS13, specific for myosin heavy chain (diluted 1/5, Cebrià et al., 1997); AA4.3, against α-tubulin to detect the dorsal epithelial cilia (diluted 1/20, Developmental Studies Hybridoma Bank); and anti-phospho-histone H3 (H3P) to detect mitotic cells (diluted 1/1000, Millipore #04-817). Alexa 488-conjugated goat anti-mouse and Alexa 568-conjugated goat anti-rabbit secondary antibodies (Molecular Probes) were used at a 1/400 and 1/1000 dilutions, respectively. Samples were mounted in SlowFade® Gold antifade (Invitrogen). Confocal laser scanning microscopy was performed with a Leica TCS-SPE and a Leica SP2.

Lectin and TUNEL staining

Lectin staining was performed essentially as described in Zayas et al. (2010). Blocking was done in 2% BSA in PBSTx. When lectin staining was done in combination with immunostaining, the lectins were added together with the secondary antibodies. Nuclear counterstaining was done with DAPI (1 μg/ml) overnight at 4 °C. Apoptotic cells were labeled as previously described (Pellettieri et al., 2010). Samples were imaged with a Leica TCS-SPE confocal laser scanning microscope.

Results

Three EGFRs in S. mediterranea

Three contigs containing open reading frames with high homology to EGFRs were isolated by tblastn searches of the planarian genome. Sequence analysis showed that all of them contained a tyrosine kinase domain highly similar to the domain found in other members of the EGFR family (see Fig. S2). Phylogenetic analysis confirmed that the planarian genes belonged to the EGFR family (see Fig. S3). These genes were named *Smed-egfr-1*, *Smed-egfr-2* and *Smed-egfr-3*.

Smed-egfrs are expressed in different cell types

Smed-egfr-1 was mainly expressed in the gut, mesenchyme and pharynx (Figs. 1A and B). In addition, *Smed-egfr-1* was weakly expressed in the eye pigment cells (arrows in inset in Fig. 1A), mouth opening (Fig. 1C) and around the region where the base of the pharynx attaches to the body mesenchyme (arrow in Fig. 1D). *Smed-egfr-2* was expressed throughout the gut but not in the pharynx (Figs. 1E–H). Finally, *Smed-egfr-3* was expressed in the pharynx, around the head margin, very weakly in the CNS (inset in Fig. 1I), and in the mesenchyme around the gut branches, in a pattern that resembles that of the neoblasts (Figs. 1I–K). After high-dose irradiation, the neoblast pool is depleted in 1–2 days and planarians die within a few weeks as they cannot sustain normal cell turnover (Bardeen and Baetjer, 1904; Reddien et al., 2005). Twelve hours after irradiation at 100 Gy, the expression of *Smed-egfr-3* in the mesenchyme around the gut branches completely disappeared (Figs. 1L–N). Eisenhoffer et al. (2008) proposed that stem cells are depleted by 24 h post-irradiation, whereas their early progeny disappears by 48 h. The fact that *Smed-egfr-3* expression disappeared very quick after irradiation, similarly to what happens to other neoblasts markers such as *Smedwi-1* and *Smedwi-2* (Reddien et al., 2005; Fig. S4) suggests that *Smed-egfr-3* was expressed in neoblasts. On the other hand, the expression of *Smed-egfr-3* in the pharynx (Fig. 1L), head margin and CNS (inset in Fig. 1L) remained, even 7 days after irradiation (data not shown), indicating that this gene was expressed in post-mitotitc differentiated cells. In contrast, *Smed-egfr-1* and *Smed-egfr-2* expression patterns did not change after irradiation (Fig. S5), suggesting that they were expressed in differentiated cells.

Smed-egfrs expression during regeneration

During posterior regeneration (head pieces regenerating the whole body), *Smed-egfr-1* was expressed in the new differentiating pharynx and posterior gut branches from 3 to 5 days after amputation (Figs. 2A, D, G, and J). During anterior regeneration (trunk pieces regenerating a new head), *Smed-egfr-1* was first observed within the blastema at day 1 (arrowhead in Fig. 2M). Between 3 and 5 days after amputation, *Smed-egfr-1* was also detected in the regenerating anterior gut branch (arrow in Fig. 2S). At day 5 of regeneration, when the regenerated eye cups are seen in live animals, *Smed-egfr-1* was strongly expressed in the new eye pigment cells (black arrowheads in Fig. 2S and T); at this stage, the newly differentiated photosensitive cells were detected with VC-1 antibody (white arrowheads in Fig. 2T). The expression of *Smed-egfr-1* in the pigment cups decreased at later stages of regeneration and was weakly detected in intact planarians.

During both posterior (Figs. 2B, E, H, and K) and anterior (Figs. 2N, Q, U, and Y) regeneration *Smed-egfr-2* was expressed in the regenerating posterior and anterior gut branches, respectively, from early stages. Finally, a strong expression of *Smed-egfr-3* was observed in both anterior and posterior 1-day blastemas (white arrowheads in Figs. 2C and O), at a stage in which an accumulation of S-phase neoblasts below the wound has been recently reported (Wenemoser and Reddien, 2010). From that moment, *Smed-egfr-3* expression was lower but still clearly detected in the differentiating pharynx and posterior gut branches during posterior regeneration (arrows in Fig. 2L), as well as the new anterior head margin (arrowheads in Figs. 2V and Z).

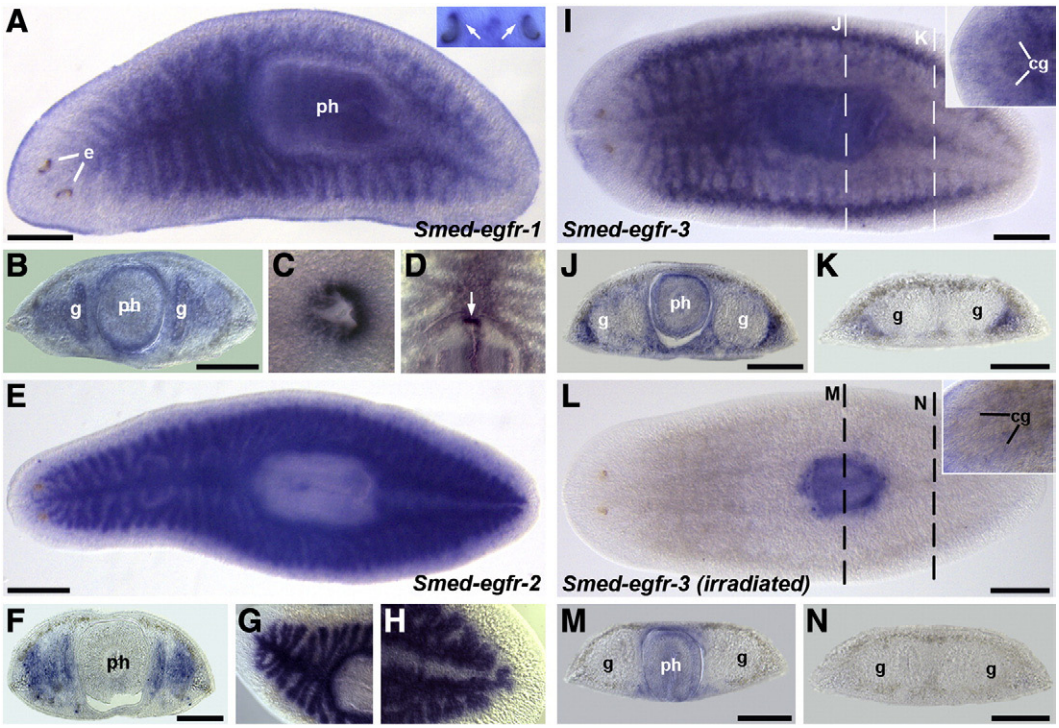

Fig. 1. Expression pattern of *Smed-egfr-1*, *Smed-egfr-2* and *Smed-egfr-3* in intact animals. (A–D) *Smed-egfr-1* is expressed throughout the mesenchyme, gut and pharynx, and in the eye pigment cells (inset in A), pharyngeal epithelia (transverse section in B), mouth opening (C) and the region where the pharynx attaches to the body mesenchyme (arrow in D). (E–H) *Smed-egfr-2* is expressed in the gut. (F) Corresponds to a transverse section. (I) *Smed-egfr-3* is expressed around the tip of the head, in the pharynx, weakly in the cephalic ganglia (inset) and in the mesenchyme around the gut branches. Dashed lines in (I) indicate the level of the transverse sections shown in (J and K). *Smed-egfr-3* is expressed around the gut branches, especially at the body lateral sides (J and K). (L) *Smed-egfr-3* expression in the mesenchyme around the gut branches is lost 12 h after irradiation at 100 Gy. Inset shows the expression in the cephalic ganglia. Dashed lines in (L) indicate the level of the transverse sections shown in (M and N). (A, C, E, G, H, I, and L) Anterior to the left. (D) Anterior to the top. e, eyes, ph, pharynx, g, gut, cg, cephalic ganglia. Scale bars, A, E, I, and L, 500 μm; B, F, J, K, M, and N, 300 μm.

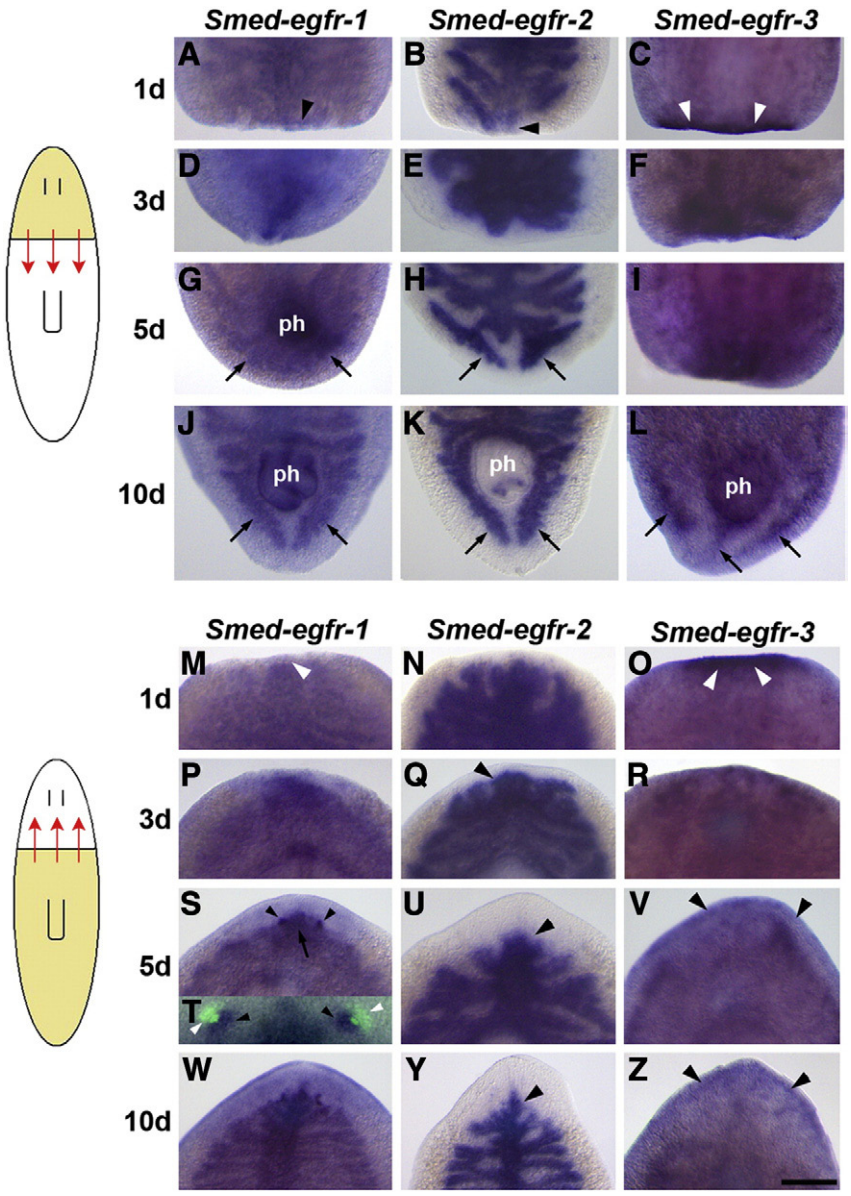

Fig. 2. Expression pattern of *Smed-egfr-1*, *Smed-egfr-2* and *Smed-egfr-3* during regeneration. Animals were cut at the prepharyngeal level (schematic drawings). (A–L) Posterior regeneration from head pieces. (M–Z) Anterior regeneration from trunk pieces. *Smed-egfr-1* is expressed in the blastema from the first day of regeneration (arrowheads in A and M). Arrows in (G, J, and S) point to expression in the regenerating gut. Black arrowheads in (S and T) point to *Smed-egfr-1* expression in eye pigment cells. White arrowheads in (T) point to the regenerating photosensitive cells after immunostaining with VC-1. *Smed-egfr-2* is expressed in the regenerating gut. Arrows in (H, K) point to the regenerating posterior gut branches. Arrowheads in (Q, U, and Y) point to the regenerating anterior gut branch. *Smed-egfr-3* is strongly upregulated within the 1-day blastemas as pointed out by white arrowheads in (C and O). Arrows in (L) point to the recovered pattern of *Smed-egfr-3* in the mesenchyme around the gut branches. Arrowheads in (V and Z) point to *Smed-egfr-3* expression at the head margin. Anterior to the top. ph, pharynx. Scale bar, 300 μm.

Smed-egfr-1 is required for eye pigment cells regeneration

After silencing *Smed-egfr-1*, regenerating trunk pieces differentiated significantly reduced pigment-cup eyes (Figs. 3A and D). Planarian eyes contain two cell types: pigment cells that constitute the eye cups, which are visible as two dark spots in the planarian head (Fig. 3A), and photosensitive cells (green in Fig. 3B), bipolar neurons that cluster around the pigment cups and send rhabdomeric projections towards them (Okamoto et al., 2005). The defects in the pigment cups (Fig. 3D) were evident from early stages and persisted throughout the regenerative process. In order to analyze whether the defects in the eye cups were due to a decrease in the number of pigment cells, a homologue of a tryptophan hydroxylase (TPH) gene was cloned. Previous studies have shown that TPH, an enzyme required for serotonin synthesis is expressed in the eye pigment cells of the planarian *Dugesia japonica* (Nishimura et al., 2007a). Similarly, *Smed-tph* was expressed in eye pigment cells (red signal in Fig. 3C). A combination of *Smed-tph* in situ and immunostaining with VC-1 clearly distinguished the two cell types (Fig. 3C). Compared to controls (Figs. 3B and G), RNAi-treated regenerating trunks generated similar numbers of photosensitive cells (67.6 ± 4.6 cells in $n = 10$ control versus 63 ± 3.31 cells in $n = 10$ RNAi-treated eyes; mean $\pm$ s.e.m.), although slightly disorganized (Figs. 3E and G). In contrast, the number of eye pigment cells was significantly reduced after *Smed-egfr-1* RNAi (16.5 ± 0.44 cells in $n = 16$ control versus 5.66 ± 0.28 cells in $n = 18$ RNAi-treated eyes; mean $\pm$ s.e.m.) (Figs. 3F and G). These results indicate that *Smed-egfr-1* is required for the proper differentiation of eye pigment cells.

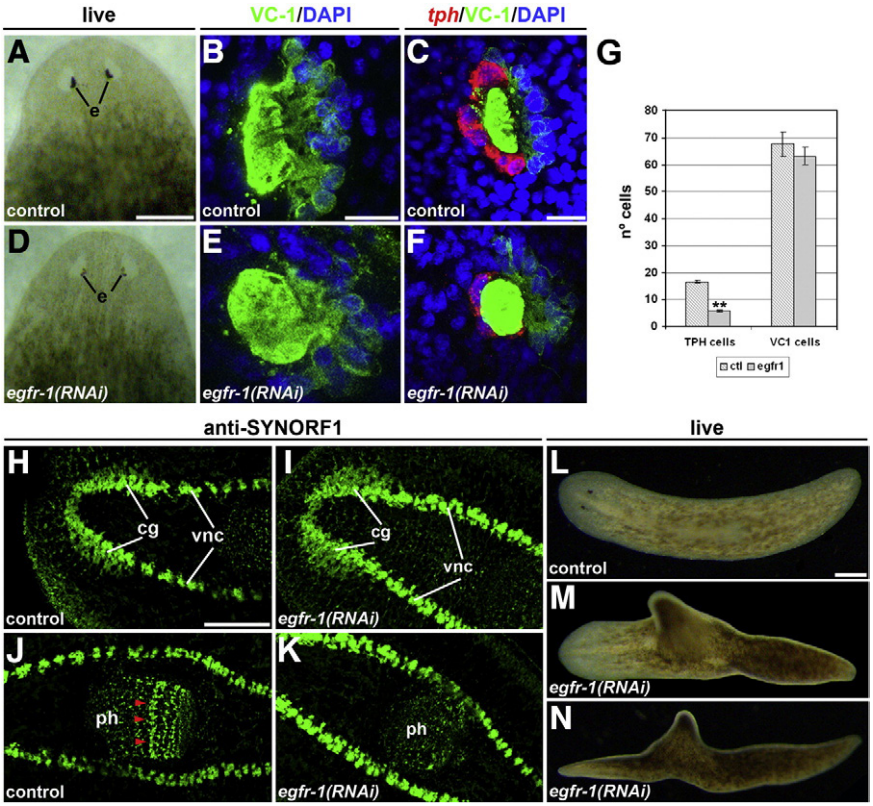

Fig. 3. *Smed-egfr-1(RNAi)* impairs eye pigment cell differentiation and induces dorsal outgrowths. (A–C) Control animals. (D–F) *Smed-egfr-1(RNAi)* animals. (A and D) Live animals, 18 days of anterior regeneration. (B and E) VC-1 immunostaining (green) and DAPI counterstaining, 8 days of regeneration. (C and F) In situ hybridization for *Smed-tph* (red) with VC-1 immunostaining (green), 10 days of regeneration. (G) Quantification of the number of *tph* and VC-1 cells in intact and *Smed-egfr-1(RNAi)* planarians, $^{**}p<0.001$ (*t*-test). (H–K) Anti-SYNORF1 immunostaining in control (H, J) and *Smed-egfr-1(RNAi)* (I, K) anterior regenerating animals, 10 days of regeneration. (L–N) Live animals, 20 days of regeneration after two rounds of amputation. (A–F) Anterior to the top. (H–N) Anterior to the left. (N) Side view. e, eyes, cg, cephalic ganglia, vnc, ventral nerve cords, ph, pharynx. Scale bars, A, D, H, and K, 400 μm; B, C, E, and F, 30 μm; L–N, 500 μm.

Smed-egfr-1 is necessary for pharynx regeneration

Immunostaining with anti-SYNORF1 (Cebrià, 2008) showed that, similarly to controls (Fig. 3H), *Smed-egfr-1* RNAi trunks regenerated apparently normal cephalic ganglia (Fig. 3I). However, the neural plexus from the original pharynges of these trunk pieces lost its typical pattern in the RNAi-treated planarians (Fig. 3K). Control pharynges showed a stereotypical neural plexus with a thick neural ring in their distal tips (red arrowheads in Fig. 3J). Remarkably, regenerating trunk pieces that went through two rounds of *Smed-egfr-1(RNAi)* and amputation developed dorsal outgrowths in the pharyngeal region (Figs. 3M and N and Table 1). As these outgrowths developed at a higher frequency after RNAi on intact animals (Table 1), their nature will be discussed in the next section. In order to better analyze the function of *Smed-egfr-1* during pharynx regeneration, we analyzed the differentiation of this organ in regenerating head pieces, which must regenerate the pharynx de novo. Twenty-five days after amputation, control head pieces regenerated morphologically normal tails and pharyngeal regions (Fig. 4A); in contrast, *Smed-egfr-1 (RNAi)* regenerating head pieces showed a widening and thickening of the new pharyngeal region that occasionally gave rise to small outgrowths (arrows in Fig. 4B and Table 1). Analysis with molecular markers showed morphogenetic defects in the regenerated pharynges of those animals. First, whereas control pieces regenerated pharynges with their stereotypical neural plexus including the distal ring (red arrowheads in Fig. 4C), *Smed-egfr-1(RNAi)* planarians regenerated smaller and more rounded pharynges with an aberrant plexus (Fig. 4D and Table 2).

Triclads, such as *S. mediterranea*, have a plicate pharynx that can be seen as a hollow muscular cylinder inside a large pharyngeal cavity (Hyman, 1951). Different tissues are present between the outer epithelium and the internal lumen (Fig. 4G; Hyman, 1951; Bueno et al., 1997). The pharyngeal lumen connects to the lumen of the gut at the base of the pharynx (Fig. 1D). Nuclear staining with DAPI showed that, whereas in control animals the pharyngeal lumen is clearly delimited and its distal end opens into the pharyngeal cavity (arrow in Fig. 4E), pharynges in *Smed-egfr-1(RNAi)* head pieces mainly developed as a solid mass of cells with no clear lumen (Fig. 4F). *Smed-egfr-1(RNAi)* pharynges also had epithelial defects. Staining with anti-SMED-βCAT2, which labels the cell junctions of the inner and outer pharyngeal epithelia (Chai et al., 2010), showed that the outer epithelial cells (Fig. 4J) had a similar morphology to the cells from the distal part of the internal epithelium (yellow asterisk and inset in Fig. 4H). In contrast, the epidermal cells in the proximal region of the internal epithelium had a

Table 1
Summary of the frequency of outgrowths after *Smed-egfr-1(RNAi)* in intact and regenerating planarians.

		Intact planarians	Regenerating planarians	
			Head pieces	Trunk pieces
Control	Normal	100% (n = 129)	97.82% (n = 138)	100% (n = 147)
	Outgrowth	0% (n = 129)	0% (n = 138)	0% (n = 147)
egfr-1(RNAi)	Normal	16.6% (n = 175)	37.62% (n = 101)	62.9% (n = 124)
	Outgrowth	83.4% (n = 175)	62.3% (n = 101)	37.1% (n = 124)

Head and trunk pieces were analyzed between 10 and 14 days of regeneration after two rounds of *egfr-1(RNAi)*. Intact animals were analyzed at week 7 of treatment, after two rounds of *egfr-1(RNAi)* during the first and third week. 100% of intact and regenerating animals treated with *egfr-1(RNAi)* showed a remarkable decreased in eye pigment cells.

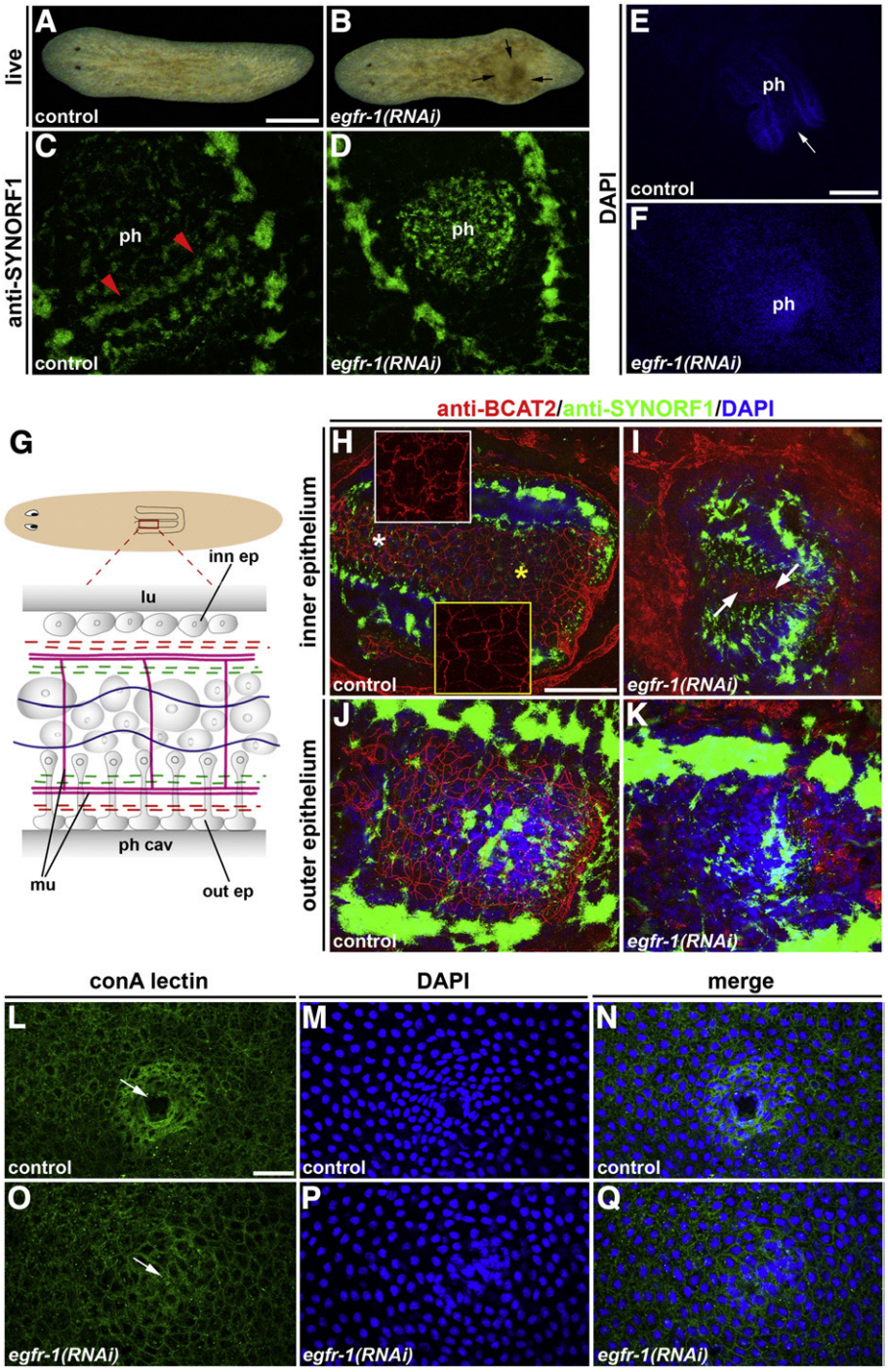

Fig. 4. *Smed-egfr-1* silencing results in defects in the regeneration of the pharynx and mouth opening. (A–B) Live animals, 25 days of regeneration. (C–D) Anti-SYNORF1 immunostaining, 13 days of regeneration. (E–F) DAPI nuclear staining, 10 days of regeneration. (G) Schematic drawing of pharynx structure (adapted from Bueno et al., 1997). Going from the pharynx cavity (ph cav) to the lumen (lu) we find the outer epithelium (out ep), subepithelial neural plexus (red discontinuous lines), muscle fibers (mu, pink), submuscular neural plexus (green discontinuous lines), mesenchyme containing different cell types, submuscular neural plexus, muscle fibers, subepithelial neural plexus and inner epithelium (inn ep). The mesenchyme is crossed by transverse muscle fibers (pink) and secretory processes (in blue). (H–K) Double anti-SMED-βCATENIN2 (red) and anti-SYNORF1 (green) immunostaining in control (H, J) and *Smed-egfr-1*(*RNAi*) (I, K) animals, 24 days of regeneration. Blue, DAPI staining. J and K correspond to different confocal planes of the same samples as H and I, respectively. White and yellow insets in (H) correspond to a higher magnification of the regions marked with white and yellow asterisks, respectively. (L–Q) Double ConA lectin (green) and DAPI staining of control (L–N) and *Smed-egfr-1*(*RNAi*) (O–Q) mouth openings, 14 days of regeneration. N and Q are merged images of L–M and O–P, respectively. Arrow in L indicates the mouth opening. Arrow in O indicates the region where the mouth should have opened. All samples correspond to regenerating head pieces. Scale bars, A–B, 500 μm; E, F, H, and K, 150 μm; L–Q, 30 μm.

different morphology, with more irregular, rougher cell junctions (white asterisk and inset in Fig. 4H). After *Smed-egfr-1*(*RNAi*), anti-SMED-βCAT2 did not label the outer epithelial cells (Fig. 4K). However, the inner epithelium was labeled even though the number and pattern of those epithelial cells was clearly abnormal compared to controls (arrows in Fig. 4I). Despite all these defects in the newly differentiated pharynges, the posterior gut branches regenerated apparently normally after *Smed-egfr-1*(*RNAi*) (data not shown).

The pharynx evaginates through a ventral mouth opening. Compared to controls (Figs. 4L–N, n = 14/16 regenerated normal

Table 2
Summary of pharynx defects observed after *Smed-egfr-1*(*RNAi*) in regenerating head pieces.

	Normal pharynges with stereotypical anti-SYNORF labeling	Smaller and rounded with abnormal anti-SYNORF labeling	Very small mass of cells and no anti-SYNORF labeling
Control	97.9% (n = 47)	2.1% (n = 47)	0% (n = 47)
egfr-1 (*RNAi*)	25% (n = 44)	56.8% (n = 44)	18.2% (n = 44)

Head pieces were analyzed between 12 and 25 days of regeneration after one round of *egfr-1*(*RNAi*). Pharynges were labeled with anti-SYNORF antibody and DAPI for nuclear counterstaining and to reveal their general structure.

mouth openings), *Smed-egfr-1*(*RNAi*) head pieces regenerated smaller, disorganized mouth openings (n = 21/35), or in many cases did not regenerate an opening (Figs. 4O–Q; n = 14/35). Overall, these results indicate that *Smed-egfr-1* is necessary for the regeneration of normal pharynges and mouth openings.

Dorsal outgrowths differentiate after Smed-egfr-1 silencing

After *Smed-egfr-1* silencing, regenerating animals occasionally developed small dorsal outgrowths (Table 1). Those outgrowths were most frequently seen in intact non-regenerating animals (arrowhead in Fig. 5B and Table 1). Around 2–3 weeks after *Smed-egfr-1*(*RNAi*), the pharyngeal regions became wider and slightly thicker, although no clear outgrowth was observed yet. After 4–5 weeks of treatment, the outgrowths began to develop, always dorsally above the pharyngeal region, and could reach a significant length after a few more weeks (Fig. 5B). In addition to these outgrowths, *Smed-egfr-1*(*RNAi*) intact planarians had reduced pigmentation of the eye cups (Fig. 5B), probably due to the inability of these animals to differentiate new eye pigment cells to sustain normal cell turnover. Despite these outgrowths, the animals did not show any sign of tissue degeneration or regression during the course of RNAi treatment.

Next, we sought to characterize those outgrowths with cell type and region-specific molecular markers. Immunostaining with anti-SYNORF1 showed that the original pharynges from *Smed-egfr-1*(*RNAi*) animals not only lost their normal neural pattern but were also displaced (Figs. 5C and D). Thus, rather than lying parallel along the anteroposterior (AP) body axis, they were perpendicular to it and their distal end pointed towards the developing dorsal outgrowth (Figs. 5D and G). In many cases, the pharynges appeared to enter the outgrowth (Fig. 5G). Anti-SMED-βCAT2 (Figs. 5E and F) showed that pharynges from *Smed-egfr-1*(*RNAi*) intact planarians were much smaller, rounded, and had a reduced lumen, and that they had the same epithelial defects as observed in regenerating head pieces. Those defects were evident before any sign of outgrowth development. In some cases, brain-like structures (arrow in Fig. 5G) and photosensitive cells (arrow in Fig. 5H) differentiated inside the outgrowths. In situ hybridizations with different markers revealed additional defects. In control animals, *Smed-sfrp-1* (Gurley et al., 2008; Petersen and Reddien, 2008) was expressed in the head tip and the most distal part of the pharynx (Fig. 5I, n = 8/8); in *Smed-egfr-1*(*RNAi*) planarians, its expression in the distal region of the pharynx appeared expanded (Fig. 5J, n = 5/8). Ectopic cells expressing the central marker *Smed-tcen* (Bueno et al., 1996; Iglesias et al., 2008) were detected in the distal part of the outgrowth (Fig. 5L, n = 3/5). Similarly, ectopic mechanosensory cells expressing *Smed-cintillo* (Oviedo et al., 2003) also differentiated inside the outgrowths (Fig. 5N, n = 1/3). In controls, *Smed-hoxD* was expressed in the posterior half of the animal, the mouth opening and also in the region where the base of the pharynx attaches to the body mesenchyme (arrowhead in Fig. 5P, n = 3/3). After *Smed-egfr-1*(*RNAi*), the expression of *Smed-hoxD* in this region was abnormally expanded (arrowheads in Fig. 5Q, n = 4/9). Immunostaining with anti-AA4.3 showed that the outgrowth displayed the typical stripe of cilia specific to the dorsal epithelium in control planarians (arrows in Fig. 5O).

Finally, immunostaining with the TMUS13 antibody (Cebrià et al., 1997) suggested that *Smed-egfr-1*(*RNAi*) animals were missing the circular muscles around the mouth opening (Figs. 5R and S). Also, the outgrowths did not have a continuous well-layered musculature underneath the epidermis, but instead individual muscle fibers and myocytes with no clear patterning differentiated inside them (Fig. 5U). Given the defects affecting the pharynx and mouth opening, we assessed whether they were still functional after long RNAi treatment. After 8 weeks of starvation, control planarians responded to food stimulus and moved quickly towards the liver paste, evaginated their pharynges and ate (see Movie 1 in the supplementary material). In contrast, *Smed-egfr-1*(*RNAi*) animals recognized and moved towards the food but were not capable of evaginating their pharynges (see Movie 2 in the supplementary material). Overall, our data show that *Smed-egfr-1*(*RNAi*) results in pharynx displacement and the development of dorsal outgrowths that have no clear AP polarity and contain a mixture of cells expressing markers for several cell types.

Hyperproliferation in Smed-egfr-1(RNAi) intact animals

Because EGFR signaling is generally involved in regulating cell proliferation in other animals and *Smed-egfr-1*(*RNAi*) resulted in significant overgrowths, we analyzed proliferation after RNAi. Whereas the proliferation rate did not significantly change after *Smed-egfr-2*(*RNAi*) and *Smed-egfr-3*(*RNAi*), a significant increase was observed after *Smed-egfr-1* silencing (Figs. 6A–D and H). This increase was observed throughout the animal (Fig. 6B), except in the pharynx and the region anterior to the eyes where there are no neoblasts and, therefore, no proliferation. Remarkably, this increase was already evident after 2 weeks of treatment (Figs. 6E–F and H), preceding any external sign of outgrowth. As planarians were starved for the whole experiment, an expected decrease in proliferation over time was observed in control, *Smed-egfr-2*(*RNAi*) and *Smed-egfr-3*(*RNAi*) planarians (Fig. 6H). In contrast, a significantly higher and rather constant proliferation rate was observed in *Smed-egfr-1*(*RNAi*) animals throughout the experiment (Fig. 6H). Although proliferative cells were also detected inside the dorsal outgrowth (arrow in Fig. 6G), they were not as numerous as in the mesenchyme outside the outgrowth.

Planarians are very plastic animals, as they can grow or degrow depending on culture conditions. Growth and degrowth depend on the balance between cell proliferation and cell death (Romero and Baguñà, 1991). Thus, planarians starved for several weeks will get smaller and smaller. After *Smed-egfr-1*(*RNAi*), intact planarians got smaller at a faster rate than controls (Fig. 6I). After only 3 weeks of treatment, *Smed-egfr-1*(*RNAi*) planarians were already significantly smaller than controls, even though their mean size was the same at the beginning of the experiment (Fig. 6I). In order to check whether this faster reduction in size could be explained by an increased cell death that would compensate for the higher proliferative rate observed in the *Smed-egfr-1*(*RNAi*) planarians, we carried out a TUNEL assay to label apoptotic cells after 9 weeks of treatment. However, no significant increase in cell death was observed [120 ± 14.01 cells/mm^2 in n = 3 controls versus 169 ± 54.71 cells/mm^2 in n = 4 *Smed-egfr-1*(*RNAi*), mean ± s.e.m].

Smed-p53 overexpression and cell lineage defects after Smed-egfr-1(RNAi)

A recent study has shown that similar dorsal outgrowths differentiate in the pharyngeal region of regenerating head and tail pieces, but not in intact planarians, after a partial silencing of *Smed-p53* (Pearson and Sánchez-Alvarado, 2010). In all cases, these outgrowths contain

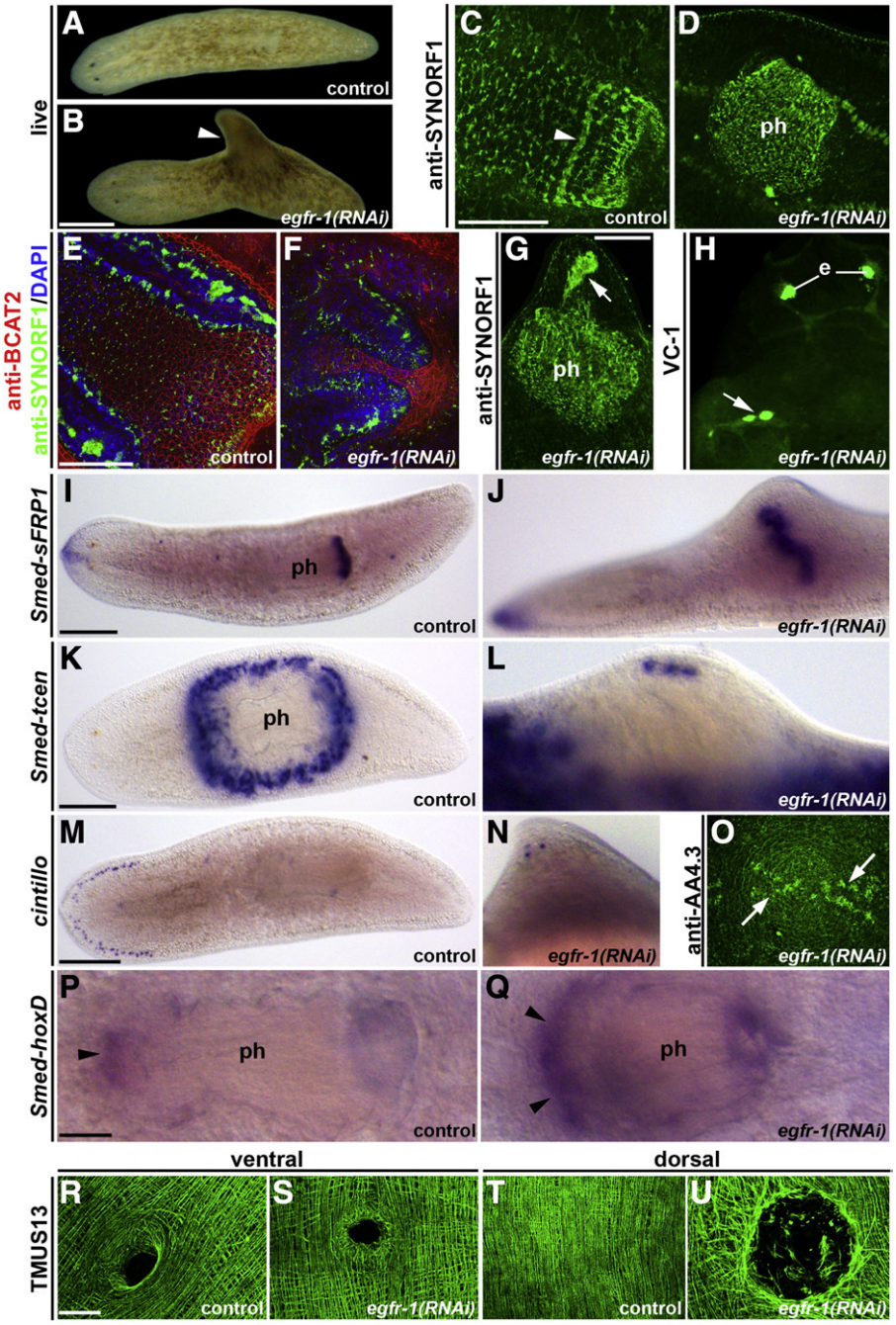

Fig. 5. Molecular characterization of the dorsal outgrowths developed after *Smed-egfr-1*(*RNAi*). (A–B) Live animals, 6 weeks of RNAi. Arrowhead in B indicates a dorsal outgrowth. (C–D) Anti-SYNORF1 immunostaining, 8 weeks of RNAi. Arrowhead in (C) indicates the stereotypical neural ring in the distal part of the pharynx. In (D), the pharynx is perpendicular to the anteroposterior body axis. (E–F) Double anti-SMED-βCATENIN2 (red) and anti-SYNORF1 (green) immunostaining in control (E) and *Smed-egfr-1*(*RNAi*) (F) pharynges, 19 days of treatment. Nuclei were labeled with DAPI. (G) Anti-SYNORF1 immunostaining showing differentiation of brain-like tissues inside the outgrowth (arrow). (H) VC-1 immunostaining showing photosensitive cells inside the outgrowth (arrow). (I–J) *Smed-sFRP-1* expression. (K–L) *Smed-tcen* expression. (M–N) *cintillo* expression. (O) Anti-AA4.3 immunostaining to show the typical pattern of dorsal epidermal cilia in the outgrowth. (P–Q) *Smed-hoxD* expression. Arrowheads point to the attachment region between the base of the pharynx and the body mesenchyme. (R–U) Body wall musculature immunostained with TMUS13. (R–S) Ventral mouth openings. (T–U) Equivalent dorsal regions. Disorganized myocytes and muscle fibers differentiated inside the outgrowth (U). (J, L, N) Side views. (G–Q) Eight weeks of RNAi. (R–U) Five weeks of RNAi. All samples correspond to intact non-regenerating animals. All panels except H (anterior to the top) show anterior to the left. ph, pharynx, e, eyes. Scale bars, A, B, I, K, and M, 500 μm; C, D, G, P, and Q, 200 μm; E, F, 150 μm; R–U, 30 μm.

multiple cells types. In intact planarians, *Smed-p53*(*RNAi*) results in an initial hyperproliferation followed by a progressive loss of mitotic cells and the death of the animals (Pearson and Sánchez-Alvarado, 2010). In contrast, *Smed-egfr-1*(*RNAi*) resulted in a sustained hyperproliferation during the whole RNAi treatment. Remarkably, the expression of *Smed-p53* appeared upregulated all throughout the animal after *Smed-egfr-1* (*RNAi*) (Fig. S6A-B). *Smed-p53* is mainly expressed in early stem cell progeny as well as in a small percentage of neoblasts (Pearson and Sánchez-Alvarado, 2010). Using *Smedwi-1* (Reddien et al., 2005) as neoblast marker, an overexpression of this gene was also observed after *Smed-egfr-1*(*RNAi*) (Fig. S6C–D).

Finally, we analyzed the effects of *Smed-egfr-1*(*RNAi*)-driven hyperproliferation and outgrowth development on a particular cell lineage of stem cell progeny (Eisenhoffer et al., 2008). For this particular lineage, we used *Smed-NB.21.11e* as a marker of early progeny and *Smed-AGAT1* as a late progeny marker (Eisenhoffer et al., 2008). In

control intact planarians *Smed-NB.21.11e* was expressed in discrete cells all throughout the ventral side (data not shown). Dorsally, *Smed-NB.21.11e* was also expressed in discrete cells uniformly distributed in the anterior half of the animal with very few cells seen post-pharyngeally (Fig. S6E). In contrast, in *Smed-egfr-1*(*RNAi*) intact planarians the dorsal expression of *Smed-NB.21.11e* was mainly concentrated in the head region whereas few cells were observed pre-pharyngeally (Fig. S6F). Higher expression, though, was seen around the pharyngeal region (Fig. S6F). No differences were observed at their ventral sides (data not shown). Transverse sections showed the presence of a higher number of *Smed-NB.21.11e*-positive cells in the mesenchyme, especially around the pharynx (Fig. S6E–F). For the late progeny marker *Smed-AGAT1* a reduction in the number of positive cells was observed at the dorsal pre-pharyngeal region (Fig. S6G–H). Finally, *Smed-AGAT1*-expressing cells were abnormally found around the digestive system of *Smed-egfr-1*(*RNAi*) planarians (Fig. S6H).

In summary, *Smed-egfr-1*(*RNAi*) results in an overexpression of *Smed-p53*, an increase of the *Smedwi-1* positive stem cell population as well as in an abnormal localization of cells expressing *Smed-NB.21.11e* and *Smed-AGAT1*, genes expressed in the non-dividing descendent cells of neoblasts in a particular lineage (Eisenhoffer et al., 2008).

Smed-egfr-3(RNAi) affects normal blastema growth

Next, we functionally characterized another EGFR homologue, *Smed-egfr-3*. After one round of *Smed-egfr-3*(*RNAi*) and amputation,

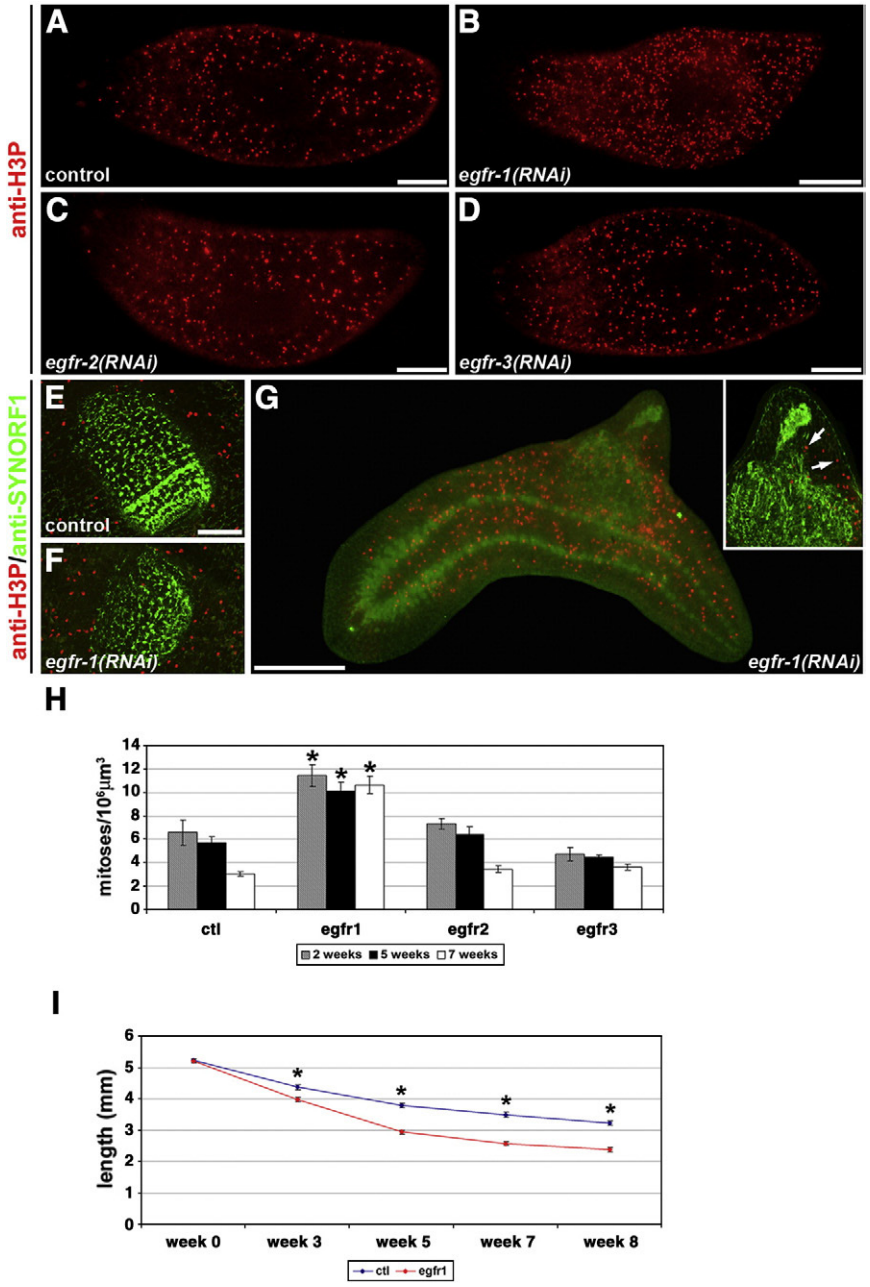

Fig. 6. Hyperproliferation and faster degrowth after *Smed-egfr-1*(*RNAi*). (A–D) Anti-H3P immunostaining after 7 weeks of RNAi. (E–G) Double immunostaining with anti-SYNORF1 (in green) and anti-H3P (in red). (E–F) Two weeks of RNAi. (G) Eight weeks of RNAi. Arrows in inset indicate mitotic cells inside the outgrowth. (H) Quantification of mitotic cells in the pre-pharyngeal region of control. At least n = 7 samples were counted per each time point. All values correspond to mean ± s.e.m., *p<0.05 (*t*-test). (I) Measurement of the size decrease upon starvation of control (0 and 3 weeks, n = 60; 5 weeks, n = 50; 7 and 8 weeks, n = 35) and *Smed-egfr-1*(*RNAi*) (0 and 3 weeks, n = 80; 5 weeks, n = 68; 7 and 8 weeks, n = 53). All values correspond to mean ± s.e.m., *p<0.05 (*t*-test). All samples correspond to intact non-regenerating animals. Scale bars, A–D, G, 500 µm; E and F, 200 µm.

all the treated animals regenerated normally. However, after two rounds of RNAi and amputation, both anterior and posterior blastemas were smaller than controls (Figs. 7A–C and S7). Planarian blastemas can be easily recognized in regenerating animals as the unpigmented white tissues that differentiate distal to the amputation surface. After 3 days of regeneration, control animals regenerated normal-sized blastemas (Fig. 7A, n = 128/131, 97.7%). However, those unpigmented anterior blastemas were significantly reduced (Fig. 7B, n = 122/261, 46.7%) or absent (Fig. 7C, n = 80/261, 30.6%) in most of the *Smed-egfr-3*(*RNAi*) animals. As *Smed-egfr-3* was expressed in irradiation-sensitive cells, the defects observed in blastema growth could be a consequence of problems in neoblast proliferation. However, the number of mitotic cells, detected with the anti-H3P antibody, was not significantly reduced after *Smed-egfr-3*(*RNAi*) (Fig. 7D–F). In contrast to other models of epimorphic regeneration such as the amphibian limb, planarian blastemas do not consist in a mass of proliferating undifferentiated cells. In planarians, upon amputation, neoblast close to the wound proliferate resulting in an accumulation of mitotic cells mainly in a narrow strip of about 300–500 μm behind the amputation plane. As regeneration proceeds the blastema grows mainly by the entry of post-mitotic neoblasts that differentiate within it in the missing structures, whereas mitotic cells are mostly restricted to the stump region outside the blastema (Newmark and Sánchez-Alvarado, 2000; Saló and Baguñà, 1984; Wenemoser and Reddien, 2010). Remarkably, the reduced 3-day blastemas from *Smed-egfr-3*(*RNAi*) animals always contained many more mitotic cells (Fig. 7E) compared to controls (Fig. 7D). After 5 days of regeneration, control animals differentiated new cephalic ganglia within the blastema (Fig. 7G); in those animals, mitotic cells were observed in the stump region (yellow arrow in Fig. 7G) and close to the brain (white arrow in Fig. 7G), but never anterior to it. In contrast, *Smed-egfr-3*(*RNAi*) animals that had reduced blastemas either differentiated small cephalic ganglia in the stump region (Fig. 7H) or the ganglia did not differentiate at all (Fig. 7I). Nevertheless, mitotic cells were abnormally located within those blastemas (arrows in Figs. 7H–I), including in front of new cephalic ganglia. Also, another stem cell marker such as *Smedwi-2* (Reddien et al., 2005) was normally present in the wound region of *Smed-egfr-3*(*RNAi*)-treated planarians despite their small blastemas (Fig. S8).

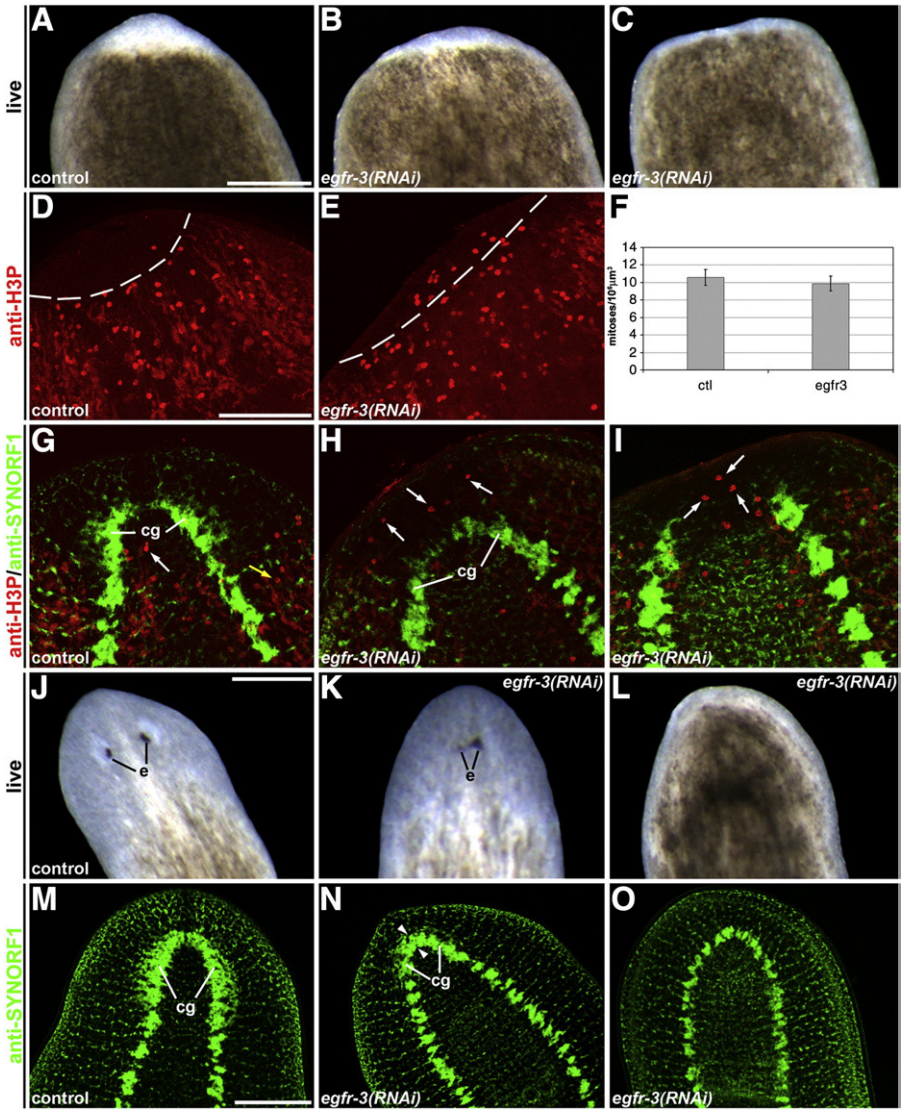

Fig. 7. Normal proliferation but abnormal blastema growth and differentiation after *Smed-egfr-3*(*RNAi*). (A–C) Live animals after 3 days of regeneration. (D–F) Anti-H3P (red) reveals no defects in proliferation rate. In contrast to controls (D), mitotic cells are found within the reduced blastemas (delineated by a discontinuous white line) of *Smed-egfr-3*(*RNAi*) planarians (E). (F) Quantification of mitotic cells in the stump region of control (10.58 ± 0.89, n = 13) and *Smed-egfr-3*(*RNAi*) (9.87 ± 0.83, n = 24) planarians. Values correspond to mean ± s.e.m. Three days of regeneration. (G–I) Double anti-SYNORF1 (green) and H3P (red) immunostaining on 5-day regenerants. Arrows indicate mitotic cells. (J–L) Live animals after 12 days of regeneration. (M–O) Anti-SYNORF1 immunostaining after 12 days of regeneration. Scale bars, A–C, 500 μm; D, E, G–I, 300 μm; J–L 400 μm; M–O, 200 μm.

After 12 days of regeneration, control animals regenerated normal anterior regions (Fig. 7J, n = 76/79, 96.2%) and cephalic ganglia (Fig. 7M). Although most *Smed-egfr-3*(*RNAi*) planarians recovered and regenerated normal anterior regions, many of those recovered blastemas showed morphological defects, mainly abnormal eyes that were fused or situated very close at the midline (Fig. 7K, n = 44/175, 25.1%). In these animals, the regenerated cephalic ganglia appeared smaller and with a thicker anterior commissure connecting the two ganglia (Fig. 7N). A number of *Smed-egfr-3*(*RNAi*) animals did not recover (Fig. 7L, n = 39/175, 22.2%) and showed more severe defects in the regeneration of their CNS (Fig. 7O). Because no abnormal phenotype was observed after one round of *Smed-egfr-3*(*RNAi*) and amputation, the variability observed on blastema growth after two rounds of RNAi and the fact that most of those treated animals recovered as regeneration proceeded, we carried out a third round of dsRNA injection and amputation. After this third round of RNAi, the animals showed a more severe phenotype compared to those observed after two rounds (Table S1). In addition, most of the animals never recovered and no blastema was observed even after 10 days of regeneration (Table S1). Importantly, and as it happens after two rounds of RNAi, those *Smed-egfr-3*(*RNAi*) animals did not display any proliferation impairment compared to controls (Fig. S9).

As *Smed-egfr-3*(*RNAi*) resulted in problems to differentiate normal blastemas despite those treated animals seemed to trigger a normal proliferative response, we checked whether the lack of normal blastemas could be due to an increased cell death. However, TUNEL assay showed that there was no increase in cell death in the wound region after 4 h, 13 h and 3 days of regeneration (Fig. S10).

Differentiation defects after Smed-egfr-3(RNAi)

As the defects observed did not seem to be caused by reduced proliferation, we assessed whether differentiation was affected after *Smed-egfr-3*(*RNAi*) (Figs. 8 and 9). Whole-mount in situ hybridizations with neural-specific genes revealed defective CNS regeneration. Thus, after 5 days of regeneration, most animals had fused cephalic ganglia at the midline, instead of normal bilateral ones, as seen with the markers *Smed-Gpas* (Iglesias et al., submitted), which is specific to the brain lateral branches (Cebrià et al., 2002b), and *Smed-th*, which labels the dopaminergic neurons (Nishimura et al., 2007b) (compare Figs. 8A and B with 8E and F, respectively). In other cases, although the regenerated cephalic ganglia appeared bilateral, expression of these neural markers was reduced (Figs. 8I and J). In the case of *Smed-Gpas*, 3-day regenerating animals showed similar results: 4/5 control planarians regenerated normal bilateral cephalic ganglia, whereas 5/8 *Smed-egfr-3*(*RNAi*) planarians regenerated fused cephalic ganglia, 2/8 were normal and 1/8 did not regenerate any CNS. After 5 days of regeneration, all controls regenerated *cintillo*-expressing cells (Fig. 8C); however, *Smed-egfr-3*(*RNAi*) animals with substantially reduced blastemas did not differentiate any *cintillo*-expressing cells within them (Fig. 8G). On the other hand, RNAi-treated animals with small blastemas differentiated *cintillo*-expressing cells (Fig. 8K). Finally, the expression of *Smed-sFRP-1* (Gurley et al., 2008) in the head anterior tip was also significantly reduced after *Smed-egfr-3*(*RNAi*) (Figs. 8H and L). Regenerating planarians analyzed at 3 days of regeneration showed similar defects: 3/4 controls were normal, whereas 4/6 *Smed-egfr-3*(*RNAi*) planarians showed a significant reduction in *Smed-sFRP-1*-expressing cells and 2/6 showed roughly a normal pattern. Planarians treated with three rounds of *Smed-egfr-3*(*RNAi*) never formed a blastema and showed a complete absence of *Smed-sFRP-1* expression even after 12 days of regeneration (Fig. S9). On the other hand, no defects using the same markers were observed after silencing *Smed-egfr-3* in intact non-regenerating planarians (Fig. S11).

Differentiation of other cell types did not appear to be affected after *Smed-egfr-3*(*RNAi*) (Fig. 9). *Smed-mag-1* labels the marginal adhesive

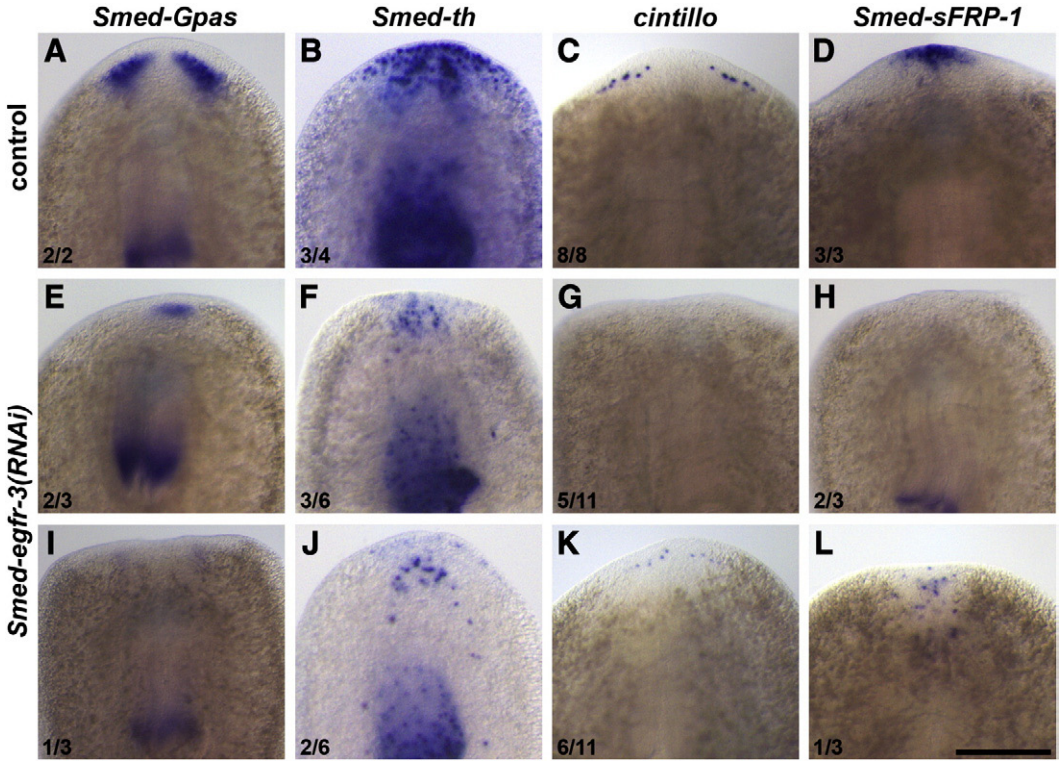

Fig. 8. Abnormal differentiation of certain cell types after *Smed-egfr-3*(*RNAi*). After 5 days of regeneration, control animals regenerated normal cephalic ganglia (*Smed-Gpas* and *Smed-th*), mechanoreceptor sensory cells (*cintillo*) and anterior distal tips (*Smed-sFRP-1*). In contrast, differentiation of these cell types was affected after *Smed-egfr-3*(*RNAi*). Scale bar, 300 μm.

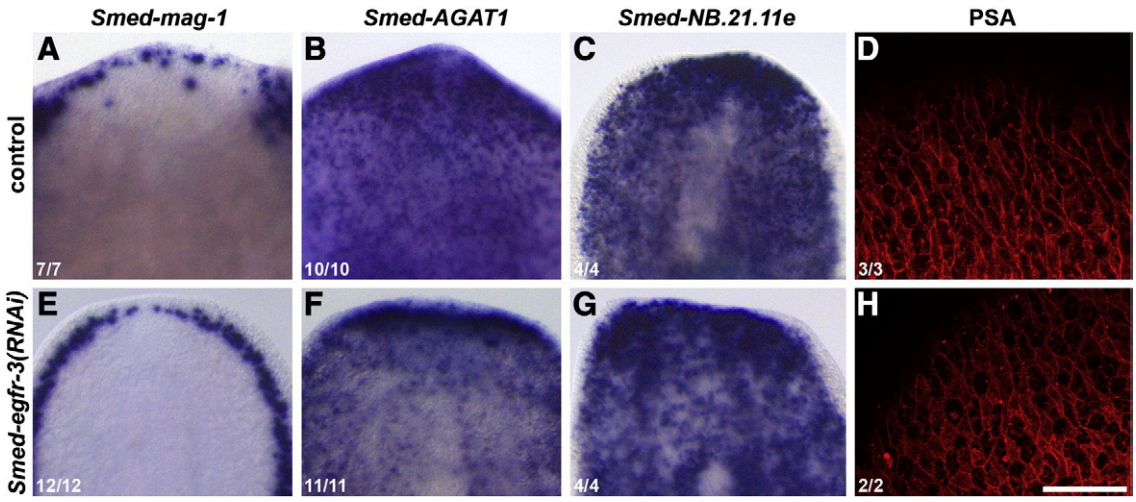

Fig. 9. Normal differentiation of certain cell types after *Smed-egfr-3*(*RNAi*). After 3 days of regeneration, *Smed-egfr-3*(*RNAi*) planarians regenerated normal patterns of *Smed-mag-1*, *Smed-AGAT1*, *Smed-NB21.11e* and lectin PSA. Scale bars, 200 μm for D–H, 300 μm for all others.

gland cells throughout the body margin except in the anterior region (Sánchez-Alvarado et al., 2002; Zayas et al., 2010). Three days after amputation, *Smed-mag-1* cells differentiated below the wound epithelium in the distal part of control (Fig. 9A) and *Smed-egfr-3*(*RNAi*) (Fig. 9E) blastemas, regardless of their sizes. Recently, *Smed-AGAT1* and *Smed-NB.21.11e* have been described as markers of late and early neoblast progeny, respectively, in a specific cell lineage (Eisenhoffer et al., 2008). After 3 days of regeneration, many *Smed-AGAT1*- and *Smed-NB.21.11e*-expressing cells were expressed within the blastemas of both control (Figs. 9B and C) and *Smed-egfr-3*(*RNAi*) (Figs. 9F and G) animals. Finally, epidermal cells staining with PSA lectin did not reveal any apparent defect in the blastema epidermis after *Smed-egfr-3*(*RNAi*) (Fig. 9H). In summary, our data show that, whereas the differentiation of some cell types was abnormal after *Smed-egfr-3*(*RNAi*) that of others was normal.

Discussion

Eye pigment cells fail to regenerate after Smed-egfr-1(RNAi)

Planarian eyes comprise pigment cells that form the eye cups and photosensitive cells that sense light. Although the origin of both cell types is not completely clear, it has recently been proposed that they could differentiate from a common precursor in *D. japonica* (Takeda et al., 2009). At early stages of regeneration, some cells are double labeled with *Djtph* and VC-1, whereas at later stages the lineages are completely separate (Takeda et al., 2009), suggesting a common origin. Since the final number of photosensitive cells is more than two-fold higher than that of the pigment cells, however, the precursors of the photosensitive cells, already expressing markers of mature cells, must go through additional rounds of proliferation after the lineages separate. Since *Smed-egfr-1*(*RNAi*) does not affect the number of photosensitive cells, *Smed-egfr-1* may be required specifically for the regeneration of the eye pigment cell lineage after its separation from a putative common precursor. *Smed-egfr-1* would be then necessary either for the differentiation of the pigment cell precursors or the proliferation of such precursors once they would separate from the photosensitive cell lineage as proposed by Takeda et al. (2009). Such a role for *Smed-egfr-1* in eye regeneration is consistent with the role of the EGFR signaling pathway in the differentiation of the different eye cell types, including pigment cells, in other systems (Freeman, 1997; Nagaraj and Banerjee, 2007).

The photosensitive cells from *Smed-egfr1*(*RNAi*) animals appear disorganized compared to controls, which suggests that a well-formed eye cup could be required to regenerate a proper eye structure. This is in agreement with proposals based on the "menashi" planarian mutant (Sato et al., 2005), in which eye pigment cells do not differentiate properly resulting in abnormal patterning of the photosensitive cells (Sato et al., 2005). Consistent with this finding, a recent report has shown that whereas eye pigment cells express *Smed-tph*, the photosensitive cells express a serotonin receptor (Saló et al., 2009), suggesting that cross-talk between these cell types may be important to regulate eye patterning and/or function. Although silencing of *Smed-tph* or the serotonin receptor does not result in any apparent defect (data not shown), a similar cross-talk may exist between currently unidentified molecules that would regulate eye patterning.

Abnormal pharynx morphogenesis after Smed-egfr-1(RNAi)

Previous studies have suggested that the planarian pharyngeal epithelium contains two types of cells. The outer epithelium and the distal part of the inner epithelium are positive for the antibody 7D8 and are formed by "insunk" (deep) cells. In contrast, the proximal part of the inner epithelium is negative for 7D8 and consists of polymorphous cells (Ishii, 1962/1963; Ishii, 1964; Kobayashi et al., 1999). Immunohistochemistry with anti-SMED-βCAT2 revealed similar staining in the outer epithelial cells and the distal inner epithelial cells, but this differed from the pattern observed in the proximal inner epithelium (Figs. 4H and J), further supporting the existence of two types of epithelial cells. These differences have led to the proposal that the inner epithelial cells have two different origins: the proximal cells would originate in the anterior part of the pharynx rudiment in close contact with the lumen of the gut and the distal cells in an invagination of a primitive slit at the posterior end of the rudiment (Kobayashi et al., 1999). As the pharynx rudiment grows and differentiates into a mature pharynx, both types of inner epithelial cells would contact each other to generate a continuous pharyngeal lumen (Kobayashi et al., 1999). After *Smed-egfr-1*(*RNAi*), the regenerated pharynges are much smaller and have a substantially reduced lumen (Figs. 4F, I and K). In parallel, anti-SMED-βCAT2 labeling is lost from the outer epithelium. Cadherin-dependent cell adhesion occurs typically through a cadherin–catenin complex (CCC) that links the membrane to the actin cytoskeleton (Gumbiner, 2005). Dynamic regulation of adhesion between epithelial cells is important to control movements such as migration, ingression or invagination. In vertebrates and *Drosophila*, EGFR associates with the CCC and may

regulate cell adhesion by phosphorylating some of its components (Dumstrei et al., 2002; Hazan and Norton, 1998; Hoschuetzky et al., 1994). Thus, for example, loss of EGFR function results in increased cell adhesion and blocks the normal invagination of the optic placode cells in *Drosophila* (Dumstrei et al., 2002). In other contexts, however, activation of EGFR signaling seems important for promoting cadherin-mediated cell adhesion (Brown et al., 2006; Jiang and Edgar, 2009). After *Smed-egfr-1*(*RNAi*), planarians regenerate abnormal pharynges with reduced lumens. Therefore, it seems reasonable to suggest that the loss of SMED-βCAT2 in the junctions of the outer epithelial cells either reveals or results in adhesion defects that lead to impairment of the morphogenetic movements that are required for proper pharynx formation.

Smed-egfr-1(RNAi) and the development of dorsal outgrowths

Smed-egfr-1 silencing results in the development of dorsal outgrowths in the pharyngeal region (Table 1). Recently, low-dose *Smed-p53*(*RNAi*) has been reported to cause a hypomorphic phenotype characterized by the development of dorsal outgrowths in regenerating head and tail pieces, just above the region where a new pharynx forms (Pearson and Sánchez-Alvarado, 2010). In both *Smed-p53*(*RNAi*) and *Smed-egfr-1*(*RNAi*), multiple cell types and tissues (brain, muscle, secretory cells, sensory cells, eyes, pharynx, gut and mitotic cells) are found within the outgrowths (Figs. 5 and 6; Pearson and Sánchez-Alvarado, 2010), although with no clear patterning along a putative AP axis. Also, anti-α-tubulin immunostaining suggests that there is no well-defined DV axis. These outgrowths (described as teratomas in Pearson and Sánchez-Alvarado, 2010) are not lethal in either case. However, whereas dorsal outgrowths also develop in regenerating trunk pieces and especially intact planarians after *Smed-egfr-1*(*RNAi*), they do not differentiate in those contexts after low-dose *Smed-p53* (*RNAi*) (Pearson and Sánchez-Alvarado, 2010).

As reported previously for *Smed-p53*(*RNAi*) (Pearson and Sánchez-Alvarado, 2010), we did not find any difference in proliferation rate compared to controls at early stages of regeneration after *Smed-egfr-1* (*RNAi*). In contrast, in intact animals there was a significant increase in the proliferation rate that was already evident 2 weeks after *Smed-egfr-1* (*RNAi*) (Fig. 6). Compared to normal-dose *Smed-p53*(*RNAi*) in intact animals, in which an initial hyperproliferation stage is followed by an almost complete loss of cell division that results in a lethal phenotype (Pearson and Sánchez-Alvarado, 2010), the hyperproliferation observed after *Smed-egfr-1*(*RNAi*) is maintained during the 8–9 weeks of treatment (Fig. 6). Despite the apparent restriction of the outgrowths to the region above the pharynx, hyperproliferation was apparent throughout the animal. Interestingly, hyperproliferation preceded the development of the outgrowth. During starvation, planarians degrow due to an imbalance between the number of newborn and dead cells during cell turnover (Romero and Baguñà, 1991). However, despite the significant hyperproliferation observed after *Smed-egfr-1*(*RNAi*) those animals degrow (in total length) much faster than controls (Fig. 6I). As this faster degrowth does not seem to be associated with an increase in cell death, one possibility is that the excess of proliferating cells might be used for the development of the outgrowths. This is further supported by the fact that animals with overall bigger outgrowths are significantly smaller than animals with overall smaller dorsal outgrowths (Table S2).

Whereas the nature and localization of these dorsal outgrowths are similar in *Smed-p53*(*RNAi*) and *Smed-egfr-1*(*RNAi*) animals, there are also some obvious differences. The most striking difference is that whereas the partial silencing of *Smed-p53* leads to the differentiation of dorsal outgrowths in regenerating head and tail pieces (Pearson and Sánchez-Alvarado, 2010), the outgrowths that develop in intact planarians after *Smed-egfr-1*(*RNAi*) differentiate in a context in which there is an overexpression of *Smed-p53* and a general hyperproliferation. Therefore, future experiments are necessary to clarify the role played by *Smed-p53* in the development of these dorsal outgrowths in the different cellular and genetic backgrounds, as well as the relationship between *Smed-p53* and *Smed-egfr-1*. What it can be concluded from the data presented here is that the silencing of *Smed-egfr-1* results in an overactivation of *Smed-p53* throughout the whole animal. Some studies in other models have suggested that p53 induces compensatory proliferation leading to hyperplastic overgrowths in some situations of cellular stress or damage (Bergmann and Steller, 2010). Therefore, a similar situation could be happening in planarians after *Smed-egfr-1*(*RNAi*), in which a hyperproliferation and overactivation of *Smed-p53* are observed together with dorsal overgrowths.

Finally, before the outgrowth develops, the original pharynges lose their normal pattern, and as the outgrowths grow these pharynges are displaced and seem to enter them. Further analyses should try to elucidate how this pharynx displacement is related to the development of the outgrowth. An interesting observation is that the expression of *Smed-hoxD* at the base of the pharynx is abnormally expanded after *Smed-egfr-1*(*RNAi*), which might argue for a role of *Smed-hoxD* in the development of the outgrowths. In summary, *Smed-egfr-1*(*RNAi*) leads to a general hyperproliferation that is associated with the development of dorsal outgrowths.

Cell fate-specific defects after Smed-egfr-3(RNAi)

Smed-egfr-3(*RNAi*) results in significantly reduced blastemas, especially during the first few days of regeneration. As *Smed-egfr-3*(*RNAi*) blastemas seem to recover as regeneration proceeds, one possibility could be that *Smed-egfr-3* silencing affects the overall growth and differentiation rate of the blastema. However, this can be ruled out because at 3 days of regeneration, cells expressing intermediate regeneration markers such as *Smed-mag-1* (first expressed within control blastemas at 2–3 days of regeneration; Zayas et al., 2010) are found within the blastema before early markers such as *Smed-Gpas* and *Smed-sFRP-1* (normally expressed between 12 h and 1 day of regeneration) are detectable. Also, TUNEL assay appears to rule out the possibility that *Smed-egfr-3*(*RNAi*) results in an increased cell death by apoptosis. Therefore, our data suggest that whereas some cell types and structures (mainly neuronal) fail to differentiate normally after *Smed-egfr-3*(*RNAi*), other non-neuronal types such as marginal gland cells and epidermal cells seem to differentiate normally. Recently, it has been reported that *Smed-CHD4* is required for the differentiation of a certain cell lineage (Scimone et al., 2010), as *Smed-CHD4*(*RNAi*) planarians fail to accumulate cells expressing the late progeny marker *Smed-AGAT1* (Eisenhoffer et al., 2008) at the wound region of regenerating animals (Scimone et al., 2010). In contrast, our results indicate that *Smed-AGAT1* cells accumulate in the wound region of *Smed-egfr-3*(*RNAi*) regenerating planarians (Fig. 9). Moreover, the silencing of *Smed-egfr-3* does not prevent either the accumulation of the early progeny marker NB.21.11e (Eisenhoffer et al., 2008) at the wound region (Fig. 9). Although the identity of the cells that express NB.21.11e and AGAT1 needs to be determined, their expression pattern and localization suggest that they are non-neuronal cell types.

The EGFR signaling pathway is involved in CNS development in other animals, including mammals, as it regulates the proliferation, differentiation, migration and survival of different populations of neural stem and progenitor cells (Aguirre et al., 2007; Doetsch et al., 2002; Gonzalez-Perez et al., 2009; O'Keeffe et al., 2009). The fact that *Smed-egfr-3* is weakly expressed in the CNS and that silencing leads to neuronal defects suggest an important role for this signaling pathway in planarian CNS regeneration. However, we cannot exclude the possibility that the defects observed in the fused and smaller cephalic ganglia after *Smed-egfr-3*(*RNAi*) are not a direct consequence of *Smed-egfr-3* loss-of-function but rather due to abnormal CNS differentiation in a much reduced blastema. Further experiments should help to address this possibility.

Another notable observation is the presence of mitotic cells within the reduced blastemas caused by *Smed-egfr-3*(*RNAi*). Recently, Wenemoser and Reddien (2010) suggested that tissue loss would induce a signal to favor differentiation of neoblast progeny near the wound. By 48 h after amputation these authors report mitotic figures within the anterior blastemas as well as a high density of *Smedwi-1*-expressing cells within them (Wenemoser and Reddien, 2010). From that moment, however, the blastema appears to be formed by cells that cease expressing *Smedwi-1* but are still positive for an antibody against the SMEDWI-1 protein; at the same time, actively cycling cells (*Smedwi-1* positive) become restricted to the base of the blastema (Wenemoser and Reddien, 2010). From these results it was proposed that from about 48 h after amputation neoblast descendants within the blastema would exit the cell cycle and would respond to differentiating signals (Wenemoser and Reddien, 2010). Thus, the presence of mitotic cells within the blastemas following *Smed-egfr-3* (*RNAi*) might be explained by an inability of neoblasts or their early descendants to moving past this stage in which they would exit the cell cycle and respond to putative differentiation signals. As not all cell types appear to be affected, distinct signals may regulate the differentiation of the different cell types in the blastema. *Smed-egfr-3* could thus control the differentiation of new neural cells during planarian regeneration. In other regenerating systems, it has been proposed that the nervous system is required for proper regeneration (Kumar et al., 2007; Miljkovic-Licina et al., 2007; Singer, 1952). Therefore, it is tempting to speculate that the reduced blastemas observed after *Smed-egfr-3*(*RNAi*) could be a consequence of abnormal neural regeneration that would affect a putative neural factor required to promote or maintain normal blastema growth.

In summary, defects in blastema growth after *Smed-egfr-3*(*RNAi*) do not seem to be caused by reduced neoblast proliferation (Fig. 7) or increased apoptotic cell death (Fig. S10). We cannot totally rule out that cell cycle stages other than the G2/M transition detected with the anti phospho histone H3 might be affected after *Smed-egfr-3*(*RNAi*); however, our results clearly indicate that the differentiation of some cell types (mainly neuronal) is affected. Future analyses should determine the exact relationship between this failure of differentiation and the much smaller blastemas regenerated after *Smed-egfr-3* (*RNAi*).

Conclusions

EGFR signaling regulates multiple intracellular target pathways affecting a wide range of biological processes. As EGFR signaling pathway is over activated in many human cancers, a lot of research is being carried out to target it for therapeutical purposes (Bianco et al., 2007; Burgess, 2008). On the other hand, in classical models of regeneration, the EGFR signaling has been shown to play different important functions. Thus, for example, it is required for the patterning of distal structures during leg regeneration in insects (Nakamura et al., 2008), for efficient liver regeneration by regulating G1–S transition during early stages (Natarajan et al., 2007), and for proper cell proliferation and migration in regenerating zebrafish (Rojas-Muñoz et al., 2009). Planarians provide an attractive framework in which to study the role of the main cell signaling pathways in regeneration and stem cell biology. Here, we report for the first time a functional characterization of EGF receptors during planarian regeneration and homeostasis. Our results indicate that EGFR signaling regulates a variety of processes during regeneration. Thus, *Smed-egfr-1* is necessary to regenerate properly eye-pigment cells and the pharynx. In addition, silencing of *Smed-egfr-1* results in hyperproliferation and development of dorsal outgrowths. On the other side, *Smed-egfr-3* is necessary for blastema growth and the differentiation of certain cell types. Because of the diversity and complexity of the phenotypes obtained, a combination of high-throughput and next-generation sequencing tools will be needed to further dissect at molecular and mechanistic levels how the silencing of each of the planarian *Smed-egfrs* leads to the defects described here.

Supplementary materials related to this article can be found online at doi:10.1016/j.ydbio.2011.03.023.

Acknowledgments

We thank the laboratories of Emili Saló and Rafael Romero for support and helpful discussions. We also thank Josep Francesc Abril for sharing bioinformatics tools, Ignacio Maeso for advice on phylogenetic analysis, Linda Stöger for cloning *Smed-AGAT1* and for establishing the lectin labeling protocol in our laboratory, Hidefumi Orii for VC-1, Teresa Adell for anti-SMED-βCAT2, R.R. for TMUS13 and María Dolores Molina, José María Martín-Durán, and David Bueno for advice on vibratome sectioning. We thank Alejandro Sánchez-Alvarado for discussion. Anti-SYNORF1 and AA4.3 monoclonal antibodies were obtained from the Developmental Studies Hybridoma Bank, University of Iowa. We thank Iain Patten for advice on English style in a version of the manuscript. S.F. is supported by an FPI fellowship (MICINN, Spain). S.B. is supported by an APIF fellowship (University of Barcelona). F.C. is a Ramón y Cajal Researcher (MICINN, Spain). This work was supported by grants BFU2008-00710 (MICINN, Spain) and 2009SGR1018 (AGAUR, Generalitat de Catalunya) to F.C.

References

Agata, K., Tanaka, C., Kobayashi, C., Kato, K., Saitoh, Y., 2003. Intercalary regeneration in planarians. Dev. Dyn. 226, 308–316.
Aguirre, A., Dupree, J.L., Mangin, J.M., Gallo, V., 2007. A functional role for EGFR signaling in myelination and remyelination. Nat. Neurosci. 10, 990–1002.
Aroian, R.V., Koga, M., Mendel, J.E., Ohshima, Y., Sternberg, P.W., 1990. The let-23 gene necessary for *Caenorhabditis elegans* vulval induction encodes a tyrosine kinase of the EGF receptor subfamily. Nature 348, 693–699.
Baguñà, J., Saló, E., Auladell, C., 1989a. Regeneration and pattern formation in planarians III. Evidence that neoblasts. Are totipotent stem cells and the source of blastema cells. Development 107, 77–86.
Baguñà, J., Saló, E., Romero, R., 1989b. Effects of activators and antagonists of the neuropeptides substance P and substance K on cell proliferation in planarians. Int. J. Dev. Biol. 33, 261–264.
Bardeen, C.R., Baetjer, F.H., 1904. The inhibitive action of the Roentgen rays on regeneration in planarians. J. Exp. Zool. 1, 191–195.
Bergmann, A., Steller, H., 2010. Apoptosis, stem cells, and regeneration. Sci. Signal. 3 (145), re8.
Bianco, R., Gelardi, T., Damiano, V., Ciardiello, F., Tortora, G., 2007. Rational bases for the development of EGFR inhibitors for cancer treatment. Int. J. Biochem. Cell Biol. 39, 1416–1431.
Birchmeier, C., 2009. ErbB receptors and the development of the nervous system. Exp. Cell Res. 315, 611–618.
Brown, K.E., Baonza, A., Freeman, M., 2006. Epithelial cell adhesion in the developing *Drosophila retina* is regulated by Atonal and the EGF receptor pathway. Dev. Biol. 300, 710–721.
Bueno, D., Baguñà, J., Romero, R., 1996. A central body region defined by a position-specific molecule in the planarian *Dugesia* (*Girardia*) *tigrina*: spatial and temporal variations during regeneration. Dev. Biol. 178, 446–458.
Bueno, D., Espinosa, L., Baguñà, J., Romero, R., 1997. Planarian pharynx regeneration in regenerating tail fragments monitored with cell-specific monoclonal antibodies. Dev. Genes Evol. 206, 425–434.
Burgess, A.W., 2008. EGFR family: structure physiology signalling and therapeutic targets. Growth Factors 26, 263–274.
Cebrià, F., 2008. Organization of the nervous system in the model planarian *Schmidtea mediterranea*: an immunocytochemical study. Neurosci. Res. 61, 375–384.
Cebrià, F., Newmark, P.A., 2005. Planarian homologs of netrin and netrin receptor are required for proper regeneration of the central nervous system and the maintenance of nervous system architecture. Development 132, 3691–3703.
Cebrià, F., Vispo, M., Newmark, P.A., Bueno, D., Romero, R., 1997. Myocyte differentiation and body wall musculatura in the planarian *Girardia tigrina*. Dev. Genes Evol. 207, 306–316.
Cebrià, F., Kobayashi, C., Umesono, Y., Nakazawa, M., Mineta, K., Ikeo, K., Gojobori, T., Itoh, M., Taira, M., Sánchez-Alvarado, A., Agata, K., 2002a. FGFR-related gene nou-darake restricts brain tissues to the head region of planarians. Nature 419, 620–624.
Cebrià, F., Nakazawa, M., Mineta, K., Ikeo, K., Gojobori, T., Agata, K., 2002b. Dissecting planarian central nervous system regeneration by the expression of neural-specific genes. Dev. Growth Differ. 44, 135–146.
Cebrià, F., Guo, T., Jopek, J., Newmark, P.A., 2007. Regeneration and maintenance of the planarian midline is regulated by a slit orthologue. Dev. Biol. 307, 394–406.
Chai, G., Ma, C., Bao, K., Zheng, L., Wang, X., Sun, Z., Saló, E., Adell, T., Wu, W., 2010. Complete functional segregation of planarian beta-catenin-1 and -2 in mediating WNT signaling and cell adhesion. J. Biol. Chem. 285, 24120–24130.

Doetsch, F., Petreanu, L., Caille, I., Garcia-Verdugo, J.M., Alvarez-Buylla, A., 2002. EGF converts transit-amplifying neurogenic precursors in the adult brain into multipotent stem cells. Neuron 36, 1021–1034.
Dumstrei, K., Wang, F., Shy, D., Tepass, U., Hartenstein, V., 2002. Interaction between EGFR signaling and DE-cadherin during nervous system morphogenesis. Development 129, 3983–3994.
Eisenhoffer, G.T., Kang, H., Sánchez-Alvarado, A., 2008. Molecular analysis of stem cells and their descendents during cell turnover and regeneration in the planarian *Schmidtea mediterranea*. Cell Stem Cell 3, 327–339.
Finn, R.D., Mistry, J., Tate, J., Coggill, P., Heger, A., Pollington, J.E., Gavin, O.L., Gunesekaran, P., Ceric, G., Forslund, K., Holm, L., Sonnhammer, E.L., Eddy, S.R., Bateman, A., 2010. The Pfam protein families database. Nucl. Acids Res. 38 (suppl 1), D211–D222.
Freeman, M., 1997. Cell determination strategies in the *Drosophila* eye. Development 124, 261–270.
Gonzalez-Perez, O., Romero-Rodriguez, R., Soriano-Navarro, M., Garica-Verdugo, J.M., Alvarez-Buylla, A., 2009. Epidermal growth factor induces the progeny of subventricular zone type B cells to migrate and differentiate into oligodendrocytes. Stem Cells 27, 2032–2043.
Gumbiner, B.M., 2005. Regulation of cadherin-mediated adhesion in morphogenesis. Nat. Rev. Mol. Cell Biol. 6, 622–634.
Gurley, K.A., Rink, J.C., Sánchez-Alvarado, A., 2008. Beta-catenin defines head versus tail identity during planarian regeneration and homeostasis. Science 319, 323–327.
Hazan, R.B., Norton, L., 1998. The epidermal growth factor receptor modulates the interaction of E-cadherin with the actin cytoskeleton. J. Biol. Chem. 273, 9078–9084.
Hoschuetzky, H., Aberle, H., Kemler, R., 1994. Beta-catenin mediates the interaction of the cadherin–catenin complex with epidermal growth factor receptor. J. Cell Biol. 127, 1375–1380.
Hyman, L.H., 1951. The Invertebrates: Platyhelminthes and Rhynchocoela. McGraw-Hill, New York.
Iglesias, M., Gómez-Skarmeta, J.L., Saló, E., Adell, T., 2008. Silencing of Smed-betacatenin1 generates radial-like hypercephalized planarians. Development 135, 1215–1221.
Ishii, S., 1962/1963. Electron microscopic observations on the planarian tissues. I. A survey of the pharynx. Fukushima J. Med. Sci. 9/10, 51–73.
Ishii, S., 1964. The ultrastructure of the outer epithelium of the planarian pharynx. Fukushima J. Med. Sci. 11, 109–125.
Jiang, H., Edgar, B.A., 2009. EGFR signaling regulates the proliferation of *Drosophila* adult midgut progenitors. Development 136, 483–493.
Kobayashi, C., Watanabe, K., Agata, K., 1999. The process of pharynx regeneration in planarians. Dev. Biol. 211, 27–38.
Kumar, A., Godwin, J.W., Gates, P.B., Garza-Garcia, A.A., Brockes, J.P., 2007. Molecular basis for the nerve dependence of limb regeneration in an adult vertebrate. Science 318, 772–777.
Larkin, M.A., Blackshields, G., Brown, N.P., Chenna, R., McGettigan, P.A., McWilliam, H., Valentin, F., Wallace, I.M., Wilm, A., Lopez, R., Thompson, J.D., Gibson, T.J., Higgins, D.G., 2007. ClustalW and ClustalX version 2. Bioinformatics 23, 2947–2948.
Livneh, E., Glazer, L., Segal, D., Schlessinger, J., Shilo, B.Z., 1985. The Drosophila EGF receptor gene homolog: conservation of both binding and kinase domains. Cell 40, 599–607.
Miljkovic-Licina, M., Chera, S., Ghila, L., Galliot, B., 2007. Head regeneration in wild-type hydra requires de novo neurogenesis. Development 134, 1191–1201.
Molina, M.D., Saló, E., Cebrià, F., 2007. The BMP pathway is essential for re-specification and maintenance of the dorsoventral axis in regenerating and intact planarians. Dev. Biol. 311, 79–94.
Nagaraj, R., Banerjee, U., 2007. Combinatorial signaling in the specification of primary pigment cells in the *Drosophila* eye. Development 134, 825–831.
Nakamura, T., Mito, T., Miyawaki, K., Ohuchi, H., Noji, S., 2008. EGFR signaling is required for re-establishing the proximodistal axis during distal leg regeneration in the cricket *Gryllus bimaculatus* nymph. Dev. Biol. 319, 46–55.
Natarajan, A., Wagner, B., Sibilia, M., 2007. The EGF receptor is required for efficient liver regeneration. Proc. Natl. Acad. Sci. U S A 104, 17081–17086.
Newmark, P.A., Sánchez-Alvarado, A., 2000. Bromodeoxyuridine specifically labels the regenerative stem cells of planarians. Dev. Biol. 220, 142–153.
Newmark, P.A., Sánchez-Alvarado, A., 2002. Not your father's planarian: a classic model enters the era of functional genomics. Nat. Rev. Genet. 3, 210–219.
Nishimura, K., Kitamura, Y., Inoue, T., Umesono, Y., Yoshimoto, K., Takeuchi, K., Taniguchi, T., Agata, K., 2007a. Identification and distribution of tryptophan hydroxylase (TPH)-positive neurons in the planarian *Dugesia japonica*. Neurosci. Res. 59, 101–106.
Nishimura, K., Kitamura, Y., Inoue, T., Umesono, Y., Sano, S., Yoshimoto, K., Inden, M., Takata, K., Taniguchi, T., Shimohama, S., Agata, K., 2007b. Reconstruction of dopaminergic neural network and locomotion function in planarian regenerates. Dev. Neurobiol. 67, 1059–1078.
Normanno, N., De Luca, A., Bianco, C., Strizzi, L., Mancino, M., Maiello, M.R., Carotenuto, A., De Feo, G., Caponigro, F., Salomon, D.S., 2006. Epidermal growth factor receptor (EGFR) signaling in cancer. Gene 366, 2–16.
O'Keeffe, G.C., Tyers, P., Aarsland, D., Dalley, J.W., Barker, R.A., Caldwell, M.A., 2009. Dopamine-induced proliferation of adult neural precursor cells in the mammalian subventricular zone is mediated through EGF. Proc. Natl. Acad. Sci. USA 106, 8754–8759.
Okamoto, K., Takeuchi, K., Agata, K., 2005. Neural projections in planarian brain revealed by fluorescent dye tracing. Zool. Sci. 22, 535–546.
Orii, H., Watanabe, K., 2007. Bone morphogenetic protein is required for dorso-ventral patterning in the planarian *Dugesia japonica*. Dev. Growth Differ. 49, 345–349.
Oviedo, N.J., Newmark, P.A., Sánchez-Alvarado, A., 2003. Allometric scaling and proportion regulation in the freshwater planarian *Schmidtea mediterranea*. Dev. Dyn. 226, 326–333.
Pearson, B.J., Sánchez-Alvarado, A., 2010. A planarian p53 homolog regulates proliferation and self-renewal in adult stem cells. Development 137, 213–221.
Pearson, B.J., Eisenhoffer, G.T., Gurley, K.A., Rink, J.C., Miller, D.E., Sánchez-Alvarado, A., 2009. Formaldehyde-based whole-mount in situ hybridization method for planarians. Dev. Dyn. 238, 443–450.
Pellettieri, J., Fitzgerald, P., Watanabe, S., Mancuso, J., Green, D.R., Sánchez-Alvarado, A., 2010. Cell death and tissue remodeling in planarian regeneration. Dev. Biol. 338, 76–85.
Petersen, C.P., Reddien, P.W., 2008. Smed-betacatenin-1 is required for anteroposterior blastema polarity in planarian regeneration. Science 319, 327–330.
Reddien, P.W., Sánchez-Alvarado, A., 2004. Fundamentals of planarian regeneration. Annu. Rev. Cell Dev. Biol. 20, 725–757.
Reddien, P.W., Oviedo, N.J., Jennings, J.R., Jenkin, J.C., Sánchez-Alvarado, A., 2005. SMEDWI-2 is a PIWI-like protein that regulates planarian stem cells. Science 310, 1327–1330.
Reddien, P.W., Bermange, A.L., Kicza, A.M., Sánchez, Alvarado A., 2007. BMP signaling regulates the dorsal planarian midline and is needed for asymmetric regeneration. Development 134, 4043–4051.
Reddien, P.W., Newmark, P.A., Sánchez-Alvarado, A., 2008. Gene nomenclature guidelines for the planarian *Schmidtea mediterranea*. Dev. Dyn. 237, 3099–3101.
Rink, J.C., Kyle, A., Gurley, K.A., Elliott, S.A., Sánchez-Alvarado, A., 2009. Planarian Hh signaling regulates regeneration polarity and links Hh pathway evolution to cilia. Science 326, 1406–1410.
Rojas-Muñoz, A., Rajadhyksha, S., Gilmour, D., van Bebber, F., Antos, C., Rodríguez Esteban, C., Nüsslein-Volhard, C., Izpisúa Belmonte, J.C., 2009. ErbB2 and ErbB3 regulate amputation-induced proliferation and migration during vertebrate regeneration. Dev. Biol. 327, 177–190.
Romero, R., Baguñà, J., 1991. Quantitative cellular analysis of growth and reproduction in freshwater planarians (Turbellaria; Tricladida). I. A cellular description of the intact organism. Invertebr. Reprod. Dev. 19, 157–165.
Sakai, F., Agata, K., Orii, H., Watanabe, K., 2000. Organization and regeneration ability of spontaneous supernumerary eyes in planarians — eye regeneration field and pathway selection by optic nerves. Zool. Sci. 17, 375–381.
Saló, E., 2006. The power of regeneration and the stem-cell kingdom: freshwater planarians (Platyhelminthes). Bioessays 28, 546–559.
Saló, E., Baguñà, J., 1984. Regeneration and pattern formation in planarians. I. The pattern of mitosis in anterior and posterior regeneration in *Dugesia* (*G*) *tigrina*, and a new proposal for blastema formation. J. Embryol. Exp. Morphol. 83, 63–80.
Saló, E., Abril, J.F., Adell, T., Cebrià, F., Eckelt, K., Fernández-Taboada, E., Handberg-Thorsager, M., Iglesias, M., Molina, M.D., Rodríguez-Esteban, G., 2009. Planarian regeneration: achievements and future directions after 20 years of research. Int. J. Dev. Biol. 53, 1317–1327.
Sánchez-Alvarado, A., Newmark, P.A., Robb, S.M., Juste, R., 2002. The *Schmidtea mediterranea* database as a molecular resource for studying platyhelminthes, stem cells and regeneration. Development 129, 5659–5665.
Sánchez-Alvarado, A., Newmark, P.A., 1999. Double-stranded RNA specifically disrupts gene expression during planarian regeneration. Proc. Natl. Acad. Sci. U S A 96, 5049–5054.
Sánchez-Alvarado, A., Tsonis, P.A., 2006. Bridging the regeneration gap: genetic insights from diverse animal models. Nat. Rev. Genet. 7, 873–884.
Sato, Y., Kobayashi, K., Matsumoto, M., Hoshi, M., Negishi, S., 2005. Comparative study of eye defective worm "menashi" and regenerating wild-type in planarian, *Dugesia ryukyuensis*. Pigment Cell Res. 18, 86–91.
Scimone, M.L., Meisel, J., Reddien, P.W., 2010. The Mi-2-like *Smed-CHD4* gene is required for stem cell differentiation in the planarian *Schmidtea mediterranea*. Development 137, 1231–1241.
Shoemaker, C.B., Ramachandran, H., Landa, A., dos Reis, M.G., Stein, L.D., 1992. Alternative splicing of the *Schistosoma mansoni* gene encoding a homologue of epidermal growth factor receptor. Mol. Biochem. Parasitol. 53, 17–32.
Singer, M., 1952. The influence of the nerve in regeneration of the amphibian extremity. Q. Rev. Biol. 27, 169–200.
Spiliotis, M., Kroner, A., Brehm, K., 2003. Identification, molecular characterization and expression of the gene encoding the epidermal growth factor receptor orthologue from the fox-tapeworm *Echinococcus multilocularis*. Gene 323, 57–65.
Takeda, H., Nishimura, K., Agata, K., 2009. Planarians maintain a constant ratio of different cell types during changes in body size by using the stem cell system. Zool. Sci. 26, 805–813.
Tamura, K., Dudley, J., Nei, M., Kumar, S., 2007. MEGA4: Molecular Evolutionary Genetics Analysis (MEGA) software version 4.0. Mol. Biol. Evol. 24, 1596–1599.
Umesono, Y., Watanabe, K., Agata, K., 1997. A planarian orthopedia homolog is specifically expressed in the branch region of both the mature and regenerating brain. Dev. Growth Differ. 39, 723–727.
Wenemoser, D., Reddien, P.W., 2010. Planarian regeneration involves distinct stem cell responses to wounds and tissue absence. Dev. Biol. 344, 979–991.
Wong, R.W., Guillaud, L., 2004. The role of epidermal growth factor and its receptors in mammalian CNS. Cytokine Growth Factor Rev. 15, 147–156.
Xian, C.J., Zhou, X.F., 2004. EGF family of growth factors: essential roles and functional redundancy in the nerve system. Front. Biosci. 9, 85–92.
Yazawa, S., Umesono, Y., Hayashi, T., Tarui, H., Agata, K., 2009. Planarian hedgehog/patched establishes anterior–posterior polarity by regulating Wnt signaling. Proc. Natl. Acad. Sci. U S A 106, 22329–22334.
Zayas, R.M., Cebrià, F., Guo, T., Feng, J., Newmark, P.A., 2010. The use of lectins as markers for differentiated secretory cells in planarians. Dev. Dyn. 239, 2888–2897.